NATIONAL ADVISORY COMMITTEE FOR AERONAUTICS

12 DEC 1947

WARTIME REPORT

ORIGINALLY ISSUED

November 1944 as
Memorandum Report L4K21

AERODYNAMIC TESTS OF AN NACA 66(215)-116, a = 0.6

AIRFOIL WITH A 0.25c SLOTTED FLAP FOR THE

FLEETWINGS XA-39 AIRPLANE

By Jones F. Cahill

Langley Memorial Aeronautical Laboratory
Langley Field, Va.

NACA

WASHINGTON

L - 629

NATIONAL ADVISORY COMMITTEE FOR AERONAUTICS

MEMORANDUM REPORT

AERODYNAMIC TESTS OF AN NACA 66(215)-116, a = 0.6

AIRFOIL WITH A 0.25c SLOTTED FLAP FOR THE

FLEETWINGS XA-39 AIRPLANE

By Jones F. Cahill

SUMMARY

Tests were conducted in the Langley two-dimensional low-turbulence tunnels on a 24-inch-chord model of the NACA 66(215)-116, a = 0.6 airfoil with a 0.25-chord slotted flap. It was desired to obtain optimum flap pivot positions for the following conditions: (a) a high maximum lift coefficient at a high flap deflection; (b) high lift coefficients with reasonably low drags at a flap deflection of 30°; and (c) a positive lift coefficient with low drags at a negative angle of attack for a flap deflection of 15°. These conditions were determined from a consideration of the landing, take-off, and strafing requirements of the airplane. Two slot entry lips were tested to find the effect of a door which closed the slot on the lower surface when the flap was retracted. Flap loads were obtained at certain configurations and the effects of external flap hinges and of the removal of the internal slot fairing skin were investigated.

The results showed that no single pivot position was the optimum for all of the specified conditions. Covering the slot by a door on the lower surface was found to cause lower drags at small flap deflections than leaving the slot open. One flap hinge was found to contribute an additional drag coefficient of 0.0002 with the flap retracted, based on an area equal to the chord squared. The removal of the interior slot fairing skin was shown to have little or no adverse effect.

INTRODUCTION

At the request of the Army Air Forces, Air Technical Service Command, tests were conducted in the Langley two-dimensional low-turbulence tunnels on a model of the inboard wing section of the Fleetwings XA-39 airplane. The section tested was a model of the NACA 66(215)-116, a = 0.6 airfoil equipped with a 25-percent-chord slotted flap. The object of the tests was to determine optimum flap pivot positions for the following conditions: (a) a high maximum lift coefficient at a high flap deflection; (b) high lift coefficients with reasonably low drags at a flap deflection of 30°; and (c) a positive lift coefficient with a low drag coefficient at a negative angle of attack for a flap deflection of 15°. Several flap pivot positions were tested with two different slot entry lips. One of the slot entry lips represented a door which closed the slot entry when the flap was retracted. Short tests were run to obtain data on the flap loads at configurations assumed to be near the optimum for each condition. Investigations were also made to find the effects of removing the internal slot fairing skin and the effects of external flap hinges.

SYMBOLS

c_l section lift coefficient

$c_{l_{max}}$ maximum section lift coefficient

$\Delta c_{l_{max}}$ increment of maximum section lift coefficient

c_d section drag coefficient

α_o section angle of attack

$c_{m_{c/4}}$ section pitching-moment coefficient

c_{r_f} section flap resultant force coefficient

θ angle between resultant force vector and flap reference line

x'   distance from flap nose to intersection of flap
          reference line and resultant force vector in
          percent of flap chord

S   pressure coefficient, defined as $-\left(\dfrac{H_O - p}{q_O}\right)$

H_O free-stream total pressurre

p   local pressure on the flap surface

q_O free-stream dynamic pressure

c   chord of airfoil

R   Reynolds number

APPARATUS AND METHODS

The model used in these tests was a 24-inch-chord
wooden model of the NACA 66(215)-116, a = 0.6 airfoil
with a 0.25c slotted flap. The flap was constructed
of metal and was provided with flush pressure orifices
at various locations along the upper and lower surfaces.
Two slot entry lips were used: one sealed the slot on
the lower surface when the flap was retracted, the other
was cut off flush with the inside surface of the slot.
During the remainder of this report, the slot entry
lip, which closed the slot on the lower surface, will
be referred to as the "long" slot entry lip and the
other as the "short" slot entry lip. The end plates
of the flap were provided with four pivot positions and
two others were added during the tests. A photograph
of the model is shown in figure 1 showing the long
slot entry lip in place and the flap at a deflection
of 50° about pivot point 1. Figure 2 is a sketch of
the main airfoil and flap showing the locations of all
six pivot points. The long slot entry lip is shown
in dotted lines. Dimensions of the flap nose shape are
also shown in figure 2. Ordinates of the plain airfoil
are given in table I. Locations of the pressure orifices
on the flap are given in table II.

Lift, drag, pitching-moment, and pressure-
distribution data were obtained by the methods outlined

in reference 1. All force and moment data have been
corrected for tunnel-wall effect by the use of the
following equations:

$$c_l = [1 - 2\beta(\gamma + \sigma) - \gamma]\; c'_l$$

$$c_d = [1 - 2\beta(\gamma + \sigma)]\; c'_d$$

$$c_m = \frac{c'_m}{1 + 2\beta(\gamma + \sigma)}$$

$$\alpha_o = (1 + \gamma)\alpha'_o$$

where

c'_l, c'_d, c'_m airfoil section coefficients measured
            in tunnel

α'_o geometric angle of attack

β factor dependent on airfoil shape

γ factor dependent on the ratio of airfoil
            chord to tunnel height

σ factor allowing for interference of
            model on tunnel static-pressure orifices,
            dependent on size and location of model

The values of the factors β, γ, and σ,
respectively, for these tests were 0.322, 0.015, and 0.002.
Tests were conducted at Reynolds numbers of approximately
2.5×10^6 in the two-dimensional low-turbulence tunnel
(designated LTT) and 6×10^6 in the two-dimensional
low-turbulence pressure tunnel (designated TDT). The
highest Mach number for any of the tests was approxi-
mately 0.140.

RESULTS AND DISCUSSION

At the outset of the tests the flow over the flap
at various configurations was investigated with tufts.
These tests showed that when the long slot entry lip

was in place, the flow over the flap was stalled at deflections greater than 20°. When the short lip was used, however, this stalling did not occur. Due to the fact that these adverse conditions existed no data were obtained at flap deflections greater than 20° using the long entry lip. "Normal" operating configurations will be assumed to signify that the long slot entry lip is used up to and including a flap deflection of 20° and the short entry lip for deflections above 20°. The long slot entry lip represents a door on the lower surface of the airplane wing which was of such a shape as to close the slot in the retracted configuration and either fold or slide into the main portion of the wing at high deflections.

Figure 3 shows the lift and drag data obtained at a Reynolds number of 2.5×10^6. These tests were in the nature of a preliminary survey. The results indicated that pivot point 4 would give the highest maximum lift at a flap deflection of 50° and the lowest drags at a 15° deflection. Pivot point 3 appeared to give the lowest drags at a 30° deflection through the intermediate lift range. Therefore, since pivot points 1 and 2 did not show the best characteristics for any of the desired conditions, they were eliminated. Pivot point 5, halfway between pivot points 3 and 4 was added at this time, apparently in an effort to combine the advantages of pivot points 3 and 4. One flap deflection about pivot point 1 was used later for the investigation of the effects of the interior slot fairing skin and the flap loads. No pitching-moment data were obtained in these tests.

Figure 4 shows the data obtained at a Reynolds number of 6×10^6 for the normal operating configurations. Moment data were obtained for pivot points 4 and 5 only. Lift and drag data for the lower deflections with the short lip are shown in figure 5.

A comparison of the drag curves at the flap-retracted configuration with the long and with the short slot entry lips (figs. 4 and 5) shows that the drag is somewhat lower with the long lip. In the low-drag range the drag coefficient with the long lip is 0.0006 lower than with the short lip at a Reynolds number of 6×10^6. The lifts, however, show no

improvement due to the use of the long lip at low deflections and, in fact, are lower in some cases.

An examination of the moment characteristics for pivot points 4 and 5 in figures 4(b) and 4(c) shows that the moments are in no case excessive. At the lower deflections, both the lift and the moment curves for the two pivot points agree fairly well. At deflections above 30° about pivot point 5, however, the flap effectiveness decreases and the moment characteristics are very nearly the same for all the higher flap deflections. For deflections about pivot point 4, both the lift and the moment characteristics show increases with flap deflection up to the maximum.

Determination of optimum configurations.- The characteristics considered desirable for this wing-flap combination were a high maximum lift at a high flap deflection; reasonably high lifts with low drags at $\delta_f = 30°$; and a positive lift coefficient with low drag at a negative angle of attack for a flap deflection of 15°. It was not considered necessary to use a single flap pivot position.

Figure 6 shows the variation in the increment of section maximum lift coefficient with flap deflection about several pivot points at both Reynolds numbers. Pivot point 4 gives the highest values of maximum lift coefficient at both Reynolds numbers. For a flap deflection of 55° about pivot point 4, the maximum lift coefficient was 2.70 at a Reynolds number of 6×10^6.

In figure 7 lift and drag characteristics at the higher lift coefficients are plotted for a flap deflection of 30° about various pivot points. The values of the drag coefficient obtained at this flap deflection above a lift coefficient of about 1.3 were not accurate and so are not included. This figure indicates that the drag coefficients at the higher lift coefficients would probably be lowest for pivot point 3. There is very little difference in the lift characteristics for the various pivot points.

A section lift coefficient of 0.18 was assumed as a reasonable point for the comparison of the various configurations at the 15° flap deflection. Lift curves are shown in figure 4(c) for the slot both sealed

(but not smoothly faired) and unsealed at a flap deflection of 15° about pivot point 5. A comparison of these two curves shows that sealing the slot moves the lift curve upward in the range useful for this flying attitude and so gives the necessary lift coefficient at a higher negative angle of attack. Figures 4(b) and 5(b) show drag polars for a flap deflection of 15° about pivot point 4 with both the long and the short slot entry lip. Using the long slot entry lip gives a drag coefficient that is 0.0003 lower than that with short slot entry lip. Completely sealing the slot entry by an extension of the slot covering door to provide a smooth contour might make even lower drag coefficients possible.

The following table gives values of the drag coefficient and angle of attack at a lift coefficient of 0.18 for a flap deflection of 15° at a Reynolds number of 6×10^6. These data are presented for various pivot positions.

Pivot	Configuration	c_l	c_d	α (deg)	Figure
3	Short lip	0.18	0.0088	$-4\frac{1}{2}$	5(a)
4	--------do.--------	.18	.0062	$-5\frac{1}{2}$	5(b)
	Long lip	.18	.0059	$-5\frac{1}{2}$	4(b)
5	Long lip (open)	.18	------	-5	4(c)
	Long lip (sealed)	.18	.0065	$-5\frac{1}{2}$	4(c)
6	--------do.--------	.18	------	$-6\frac{1}{2}$	10

From these values it is observed that pivot point 4 combined with the long slot entry lip would give the lowest drag coefficient at a fairly high negative angle of attack. When the flap is pivoted at this point its path is such that its upper surface remains in contact with the upper slot lip at all deflections up to 20°. The smooth contour that this affords may account for the lower drag. Thus, for the 15° flap deflection, pivot point 4 would give the lowest drag coefficient at a lift coefficient of 0.18

while pivot point 6 would give the desired lift coefficient at the highest negative angle of attack.

Flap loads.- It was desired to obtain data on the flap loads for design purposes. The configurations tested were not the optimum for each of the desired flight attitudes but it was assumed that the data obtained would provide indications of the loads to be expected at the better configurations. Pivot point 6 was added at this time, since it was expected to provide better characteristics for the 15° flap deflection. Time was not available, however, for more complete tests of the flap pivoted at this point.

Pressure-distribution data are presented in table III for flap deflections of 15° about pivot point 6, 30° about pivot point 1, and 50° about pivot point 4. Data were obtained with the slot completely sealed and faired on the lower surface for the 15° flap deflection and completely open with the short slot entry lip at the other two configurations. The pressure distributions are presented in terms of the pressure coefficient S. The data for the 30° and 50° deflections were obtained at a Reynolds number of 2.5 × 10^6 and the data for the 15° deflection were obtained at a Reynolds number of 6 × 10^6.

Resultant force coefficient vectors are shown in figure 8. The resultant force coefficients are plotted against section lift coefficient in figure 9 and section lift coefficients are plotted against section angle of attack in figure 10. Values of the resultant force coefficients, their points of intersection, and angles of incidence with the flap reference line are listed in table IV. The flap reference line coincides with the chord line of the undisturbed airfoil. The resultant force coefficients were obtained from integrations of the pressure coefficients plotted against their positions on lines parallel and perpendicular to the flap reference line.

Data from table IV for the flap deflection of 15°, when plotted, show that between the angles of attack of -8° and -4° the flow separates from the rear portion of the upper surface and the pressure peak near the leading edge drops abruptly. This explains the sudden change in position and direction of the resultant force vectors between these angles of attack.

Between 0° and 1°, this flap stall becomes almost complete causing the sharp drop in the resultant force coefficient and the break in the lift curve.

Effect of removing the interior slot fairing skin.- These tests were run to investigate the effect of eliminating the skin on the inside surface of the slot. The model was modified for these tests as shown in the sketch of figure 11.

Figure 12 shows section characteristics of the model, both before and after the modifications, were made to the slot fairing. Data are presented for the flap retracted, deflected 30° about pivot point 1, and deflected 50° about pivot point 4. These data were obtained at a Reynolds number of 6 × 10⁶.

There is but slight difference between the lift characteristics of the model with the slot skin removed and in the original condition. The only adverse effects on lift due to the removal of the skin are a slight decrease in maximum lift with the flap retracted and at the 50° deflection. An increase in the maximum lift at the 30° deflection and in the lift coefficients at the lower angles of attack at the 50° deflection were noted.

In the flap retracted configuration, removal of the slot skin increased the drag at all but the higher positive lift coefficients. Above a lift coefficient of about 0.6, there was a slight decrease in the drag coefficient when the slot fairing skin was removed. The increase in the minimum drag coefficient amounts to about 0.0002. From this standpoint it might be considered advisable to retain the slot fairing skin. If the slot covering door is used in the flap-retracted configuration, however, this drag increment would not be experienced. At the 30° deflection the drags were lower throughout the entire range of lift coefficients tested when the skin was removed.

The pitching-moment coefficients do not change appreciably with the slot configuration. It should be noted that the pitching-moment curve for the original condition with the flap retracted is given for the long slot entry lip configuration. All the other curves are given for the short lip configuration.

Drag increment due to external flap hinges.-
Spanwise drag surveys are shown in figure 13 for the
model both with and without external flap hinges. A
sketch of the hinges is also shown on the figure. The
small waves in the curves are probably due to the
spanwise flow in the slot. The waves were not eliminated,
however, when thin chordwise dams were placed in the slot.
The additional drag coefficient caused by one hinge
amounts to 0.0002 when based on an area equal to the
airfoil chord squared.

CONCLUSIONS

Tests were conducted in the Langley two-dimensional
low-turbulence tunnels on a 24-inch-chord model of the
NACA 66(215)-116, a = 0.6 airfoil equipped with a
0.25c slotted flap. The results obtained provided the
following conclusions:

1. Covering the slot entry with a flush door gave
minimum drag coefficients lower than the no-door con-
figuration by 0.0006 at a Reynolds number of 6.0 × 10⁶
with the flap retracted.

2. The highest maximum lift coefficient measured
was 2.70 and was obtained with a flap deflection of
55° about pivot point 4.

3. The results indicated that the lowest drag at
high lift coefficients for the 30° flap deflection would
be obtained with pivot point 3.

4. At a flap deflection of 15°, pivot point 4
appeared to give the lowest drag at a lift coefficient
of 0.18 while pivot point 6 gave this lift coefficient
at the highest negative angle of attack.

5. Few adverse effects were incurred as a result
of removing the interior slot fairing skin provided the
slot is covered by a door on the lower surface when
the flap is retracted.

6. The external flap hinges tested gave an increment in the drag coefficient based on an area equal to the airfoil chord squared of 0.0002 for one hinge.

Langley Memorial Aeronautical Laboratory
    National Advisory Committee for Aeronautics
        Langley Field, Va., November 21, 1944

REFERENCE

1. Jacobs, Eastman N., Abbott, Ira H., and Davidson, Milton: Preliminary Low-Drag-Airfoil and Flap Data from Tests at Large Reynolds Numbers and Low Turbulence, and Supplement. NACA ACR, March 1942.

TABLE I

Ordinates for NACA 66(215)-116, a = 0.6 Airfoil
(Stations and ordinates in percent of chord)

Upper Surface		Lower Surface	
Station	Ordinate	Station	Ordinate
0	0	0	0
0.435	1.214	0.565	-1.150
0.678	1.462	0.822	-1.370
1.170	1.823	1.330	-1.683
2.408	2.498	2.592	-2.254
4.897	3.498	5.103	-3.082
7.392	4.286	7.608	-3.726
9.890	4.969	10.110	-4.281
14.894	6.054	15.106	-5.154
19.903	6.895	20.097	-5.827
24.916	7.554	25.084	-6.346
29.931	8.052	30.069	-6.738
34.949	8.401	35.051	-7.009
39.968	8.633	40.032	-7.185
44.989	8.734	45.011	-7.260
50.011	8.694	49.989	-7.220
55.037	8.502	54.963	-7.058
60.070	8.113	59.930	-6.737
65.096	7.459	64.904	-6.203
70.099	6.519	69.901	-5.419
75.091	5.429	74.909	-4.503
80.074	4.218	79.926	-3.478
85.053	2.995	84.947	-2.451
90.030	1.763	89.970	-1.411
95.011	0.679	94.989	-0.514
100	0	100	0

NATIONAL ADVISORY
COMMITTEE FOR AERONAUTICS

TABLE II

Locations of Flap Pressure Orifices
(Stations given in percent of flap chord)

Upper Surface		Lower Surface	
Tube No.	Station	Tube No.	Station
1	3.2	1	7.3
2	10.2	2	23.3
3	20.8	3	31.4
4	32.4	4	42.9
5	43.7	5	56.2
6	56.4	6	84.5
7	67.8		

TABLE III

Pressure Distributions

Pressure coefficient "S" for tube nos.:

α deg	Upper 1	2	3	4	5	6	7	Lower 1	2	3	4	5	6

$\delta_f = 15^\circ$; pivot point 6; slot sealed on lower surface

α deg	Upper 1	2	3	4	5	6	7	Lower 1	2	3	4	5	6
-16.24	1.578	1.580	1.580	1.372	1.136	.984	.907	.941	.907	.897	.867	.848	.824
-12.18	1.607	1.603	1.608	1.451	1.167	1.010	.916	.818	.794	.798	.778	.765	.765
- 8.12	1.717	1.717	1.719	1.451	1.212	1.041	.929	.705	.717	.741	.746	.728	.752
- 4.06	1.369	1.367	1.375	1.325	1.248	1.205	1.161	.524	.692	.746	.747	.746	.815
0	1.305	1.306	1.311	1.275	1.225	1.203	1.199	.354	.655	.723	.723	.728	.773
1.02	1.232	1.232	1.237	1.221	1.209	1.198	1.205	.367	.695	.750	.751	.762	.869
4.06	1.253	1.253	1.257	1.225	1.198	1.202	1.209	.335	.665	.731	.731	.747	.867
8.12	1.258	1.259	1.286	1.220	1.202	1.203	1.209	.352	.631	.697	.702	.724	.857
12.18	1.286	1.291	1.302	1.242	1.237	1.243	1.259	.268	.614	.680	.687	.713	.861
16.24	1.374	1.379	1.368	1.319	1.314	1.314	1.314	.257	.615	.681	.692	.724	.890
20.30	1.802	1.792	1.808	1.914	1.893	1.849	1.813	.275	.769	.867	.901	.937	1.170

$\delta_f = 30^\circ$; pivot point 1; short slot entry lip

α deg	Upper 1	2	3	4	5	6	7	Lower 1	2	3	4	5	6
-12.18	1.436	1.809	2.700	2.113	1.476	1.262	1.181	.161	.232	.357	.468	.548	.752
- 7.10	1.909	1.968	3.151	2.534	1.891	1.296	1.135	.062	.224	.331	.429	.492	.679
- 2.03	1.728	1.925	3.113	2.355	1.599	1.304	1.169	.048	.202	.315	.395	.464	.659
3.04	1.921	1.992	2.750	1.950	1.518	1.306	1.224	.067	.181	.286	.369	.448	.655
6.09	1.942	2.129	2.992	2.308	1.540	1.218	1.056	.069	.161	.252	.335	.411	.611

$\delta_f = 50^\circ$; pivot point 4; short slot entry lip

α deg	Upper 1	2	3	4	5	6	7	Lower 1	2	3	4	5	6
-10.15	1.458	2.673	1.990	1.500	1.468	1.470	1.474	.714	.008	.067	.210	.331	.710
- 5.08	1.665	3.052	2.488	1.500	1.448	1.458	1.458	.661	.028	.101	.210	.315	.677
- 1.02	1.863	3.052	2.581	1.460	1.403	1.405	1.415	.615	.024	.087	.185	.290	.631
3.04	1.923	3.032	2.573	1.435	1.377	1.367	1.379	.575	.012	.073	.167	.270	.589
6.09	1.964	3.018	2.556	1.438	1.367	1.363	1.375	.558	.014	.067	.149	.248	.571

TABLE IV

Resultant Force Coefficients

$\delta_f = 15°$; pivot point 6; slot sealed on lower surface

α deg	c_l	c_{r_f}	θ deg	x'
-16.24	-.809	.318	124°56'	29.07
-12.18	-.407	.414	121°20'	30.79
-8.12	.052	.511	119°34'	32.08
-4.06	.381	.476	105°50'	41.72
0	.769	.501	102°56'	42.92
1.02	.776	.431	100°58'	43.14
4.06	1.032	.463	100°58'	42.67
8.12	1.415	.472	102°12'	42.24
12.18	1.649	.520	100°52'	42.67
16.24	1.730	.574	102°04'	42.17
20.30	1.187	.816	99°28'	42.53

$\delta_f = 30°$; pivot point 1; short slot entry lip

α deg	c_l	c_{r_f}	θ deg	x'
-12.18	-.026	1.109	98°50'	34.83
-7.10	.617	1.273	100°60'	33.53
-2.03	1.186	1.237	102°12'	34.96
3.04	1.656	1.200	103°04'	35.42
6.09	1.991	1.258	104°48'	32.62

$\delta_f = 50°$; pivot point 4; short slot entry lip

α deg	c_l	c_{r_f}	θ deg	x'
-10.15	.509	1.184	101°56'	41.65
-5.08	1.098	1.289	104°14'	40.60
-1.02	1.537	1.352	103°56'	39.38
3.04	1.957	1.359	105°24'	38.73
6.09	2.307	1.396	105°40'	40.05

θ = angle between flap reference line and resultant
force vector

x' = distance from nose to intersection of flap reference
line and resultant force vector in percent of flap
chord
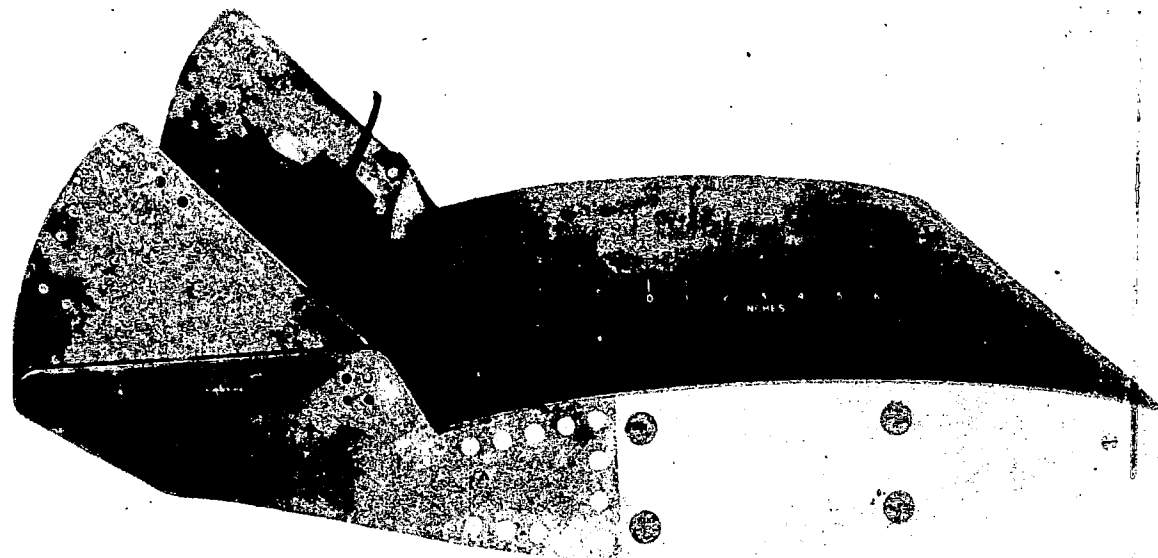
Figure 1.- NACA 66(215)-116, a = 0.6 airfoil with a 0.25-chord slotted flap. Flap deflected 50° about pivot point 1: long entry lip configuration.

0.250

0.070 R

0.023

0.035

0.018 R

0.181

0.231

All dimensions are given in fractions of
the plain wing chord.
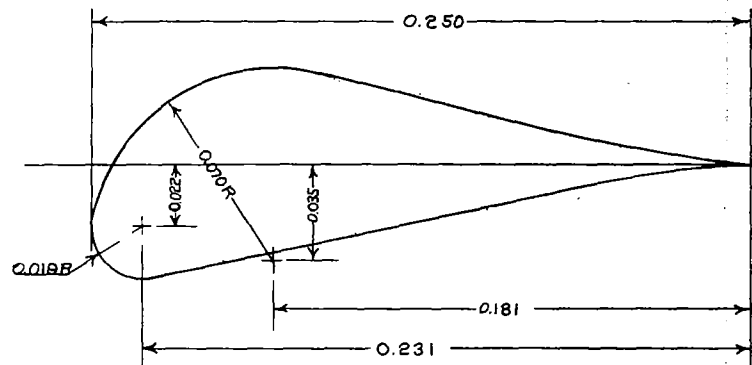
Dimensions of flap nose shape

0.0396

0.00800

0.01006

6 3 5 4

1 2

0.1752

0.1856

0.1960

0.2235
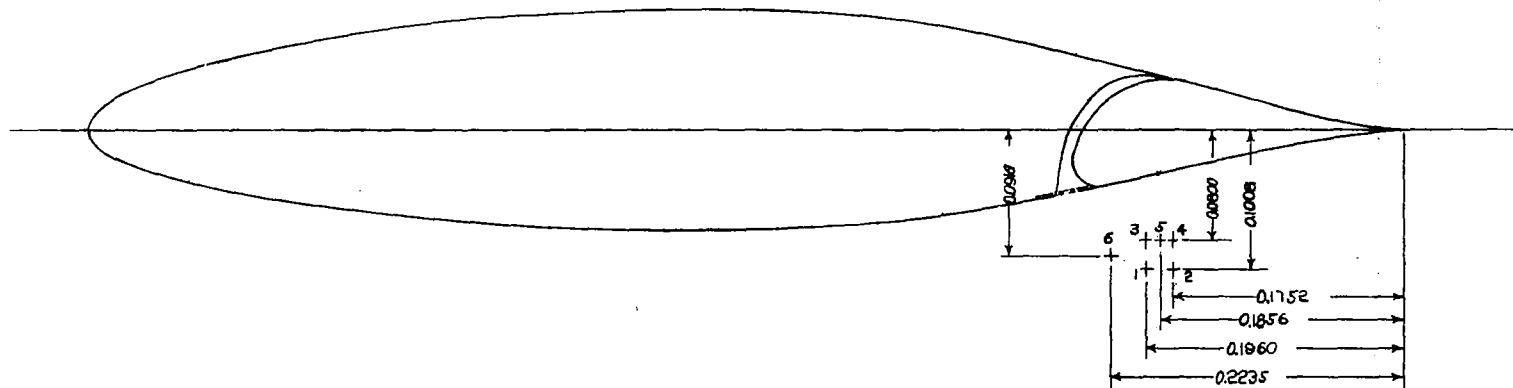
NATIONAL ADVISORY
COMMITTEE FOR AERONAUTICS

Figure 2.- NACA 66(215)-116, a = 0.6 airfoil with a 0.25-chord slotted
flap, showing location of various pivot points.
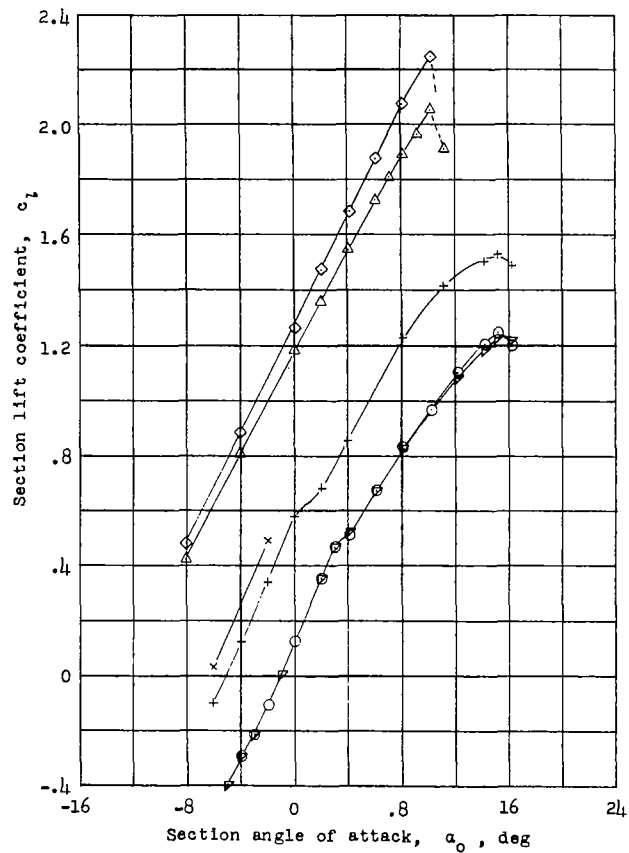
(a) Pivot point 1

Figure 3.- Lift and drag characteristics of an NACA 66(215)-116, a = 0.6
airfoil with a 0.25-chord slotted flap using various pivot points;
R, 2.5 × 10^6 (approx.).
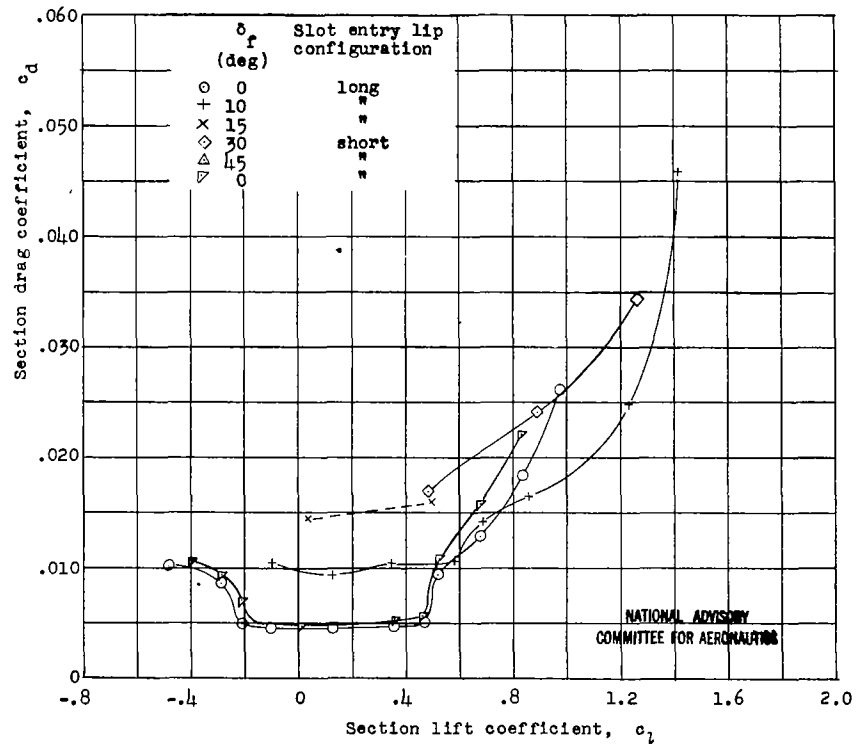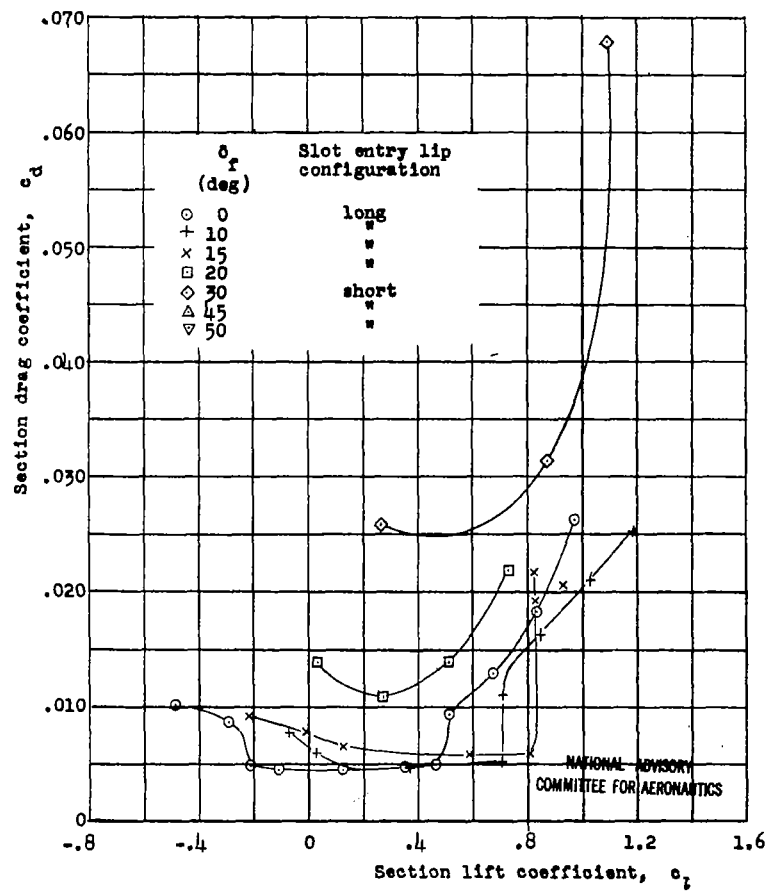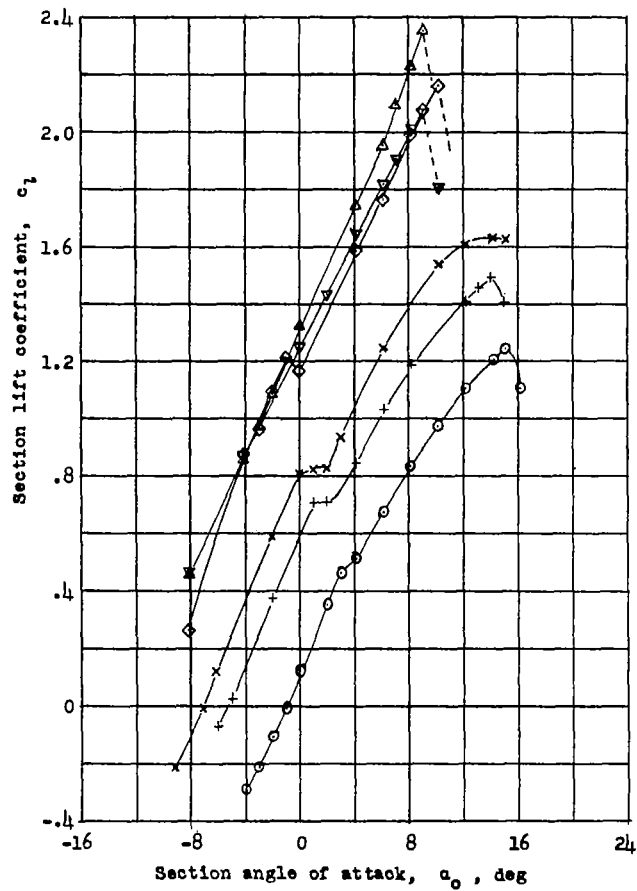
Figure 3.- Continued.   (b) Pivot point 2
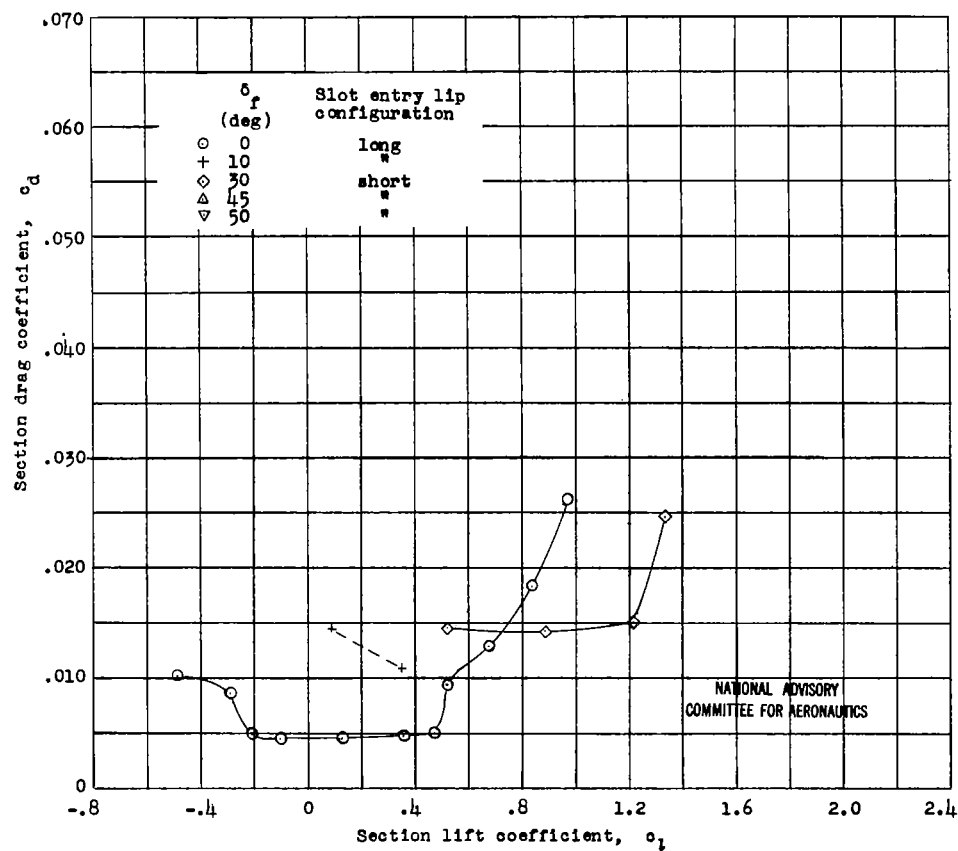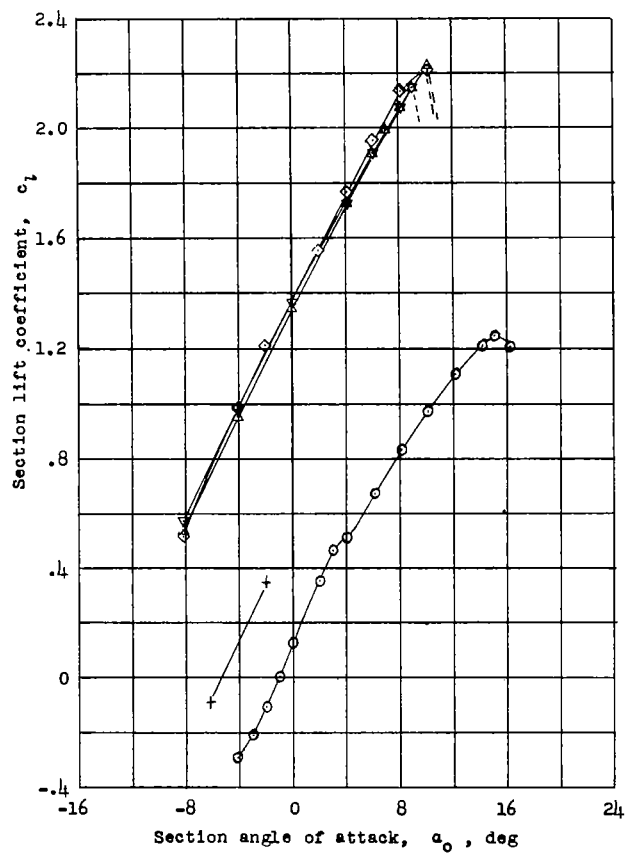
Figure 3 .- Continued.   (c) Pivot point 3
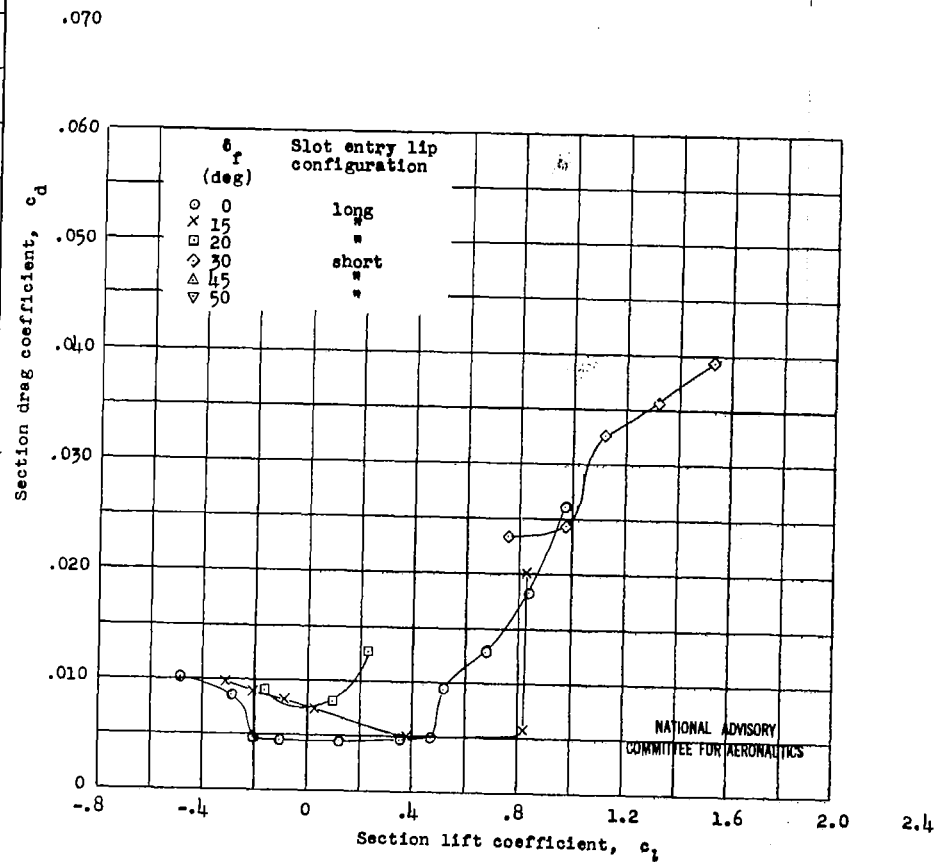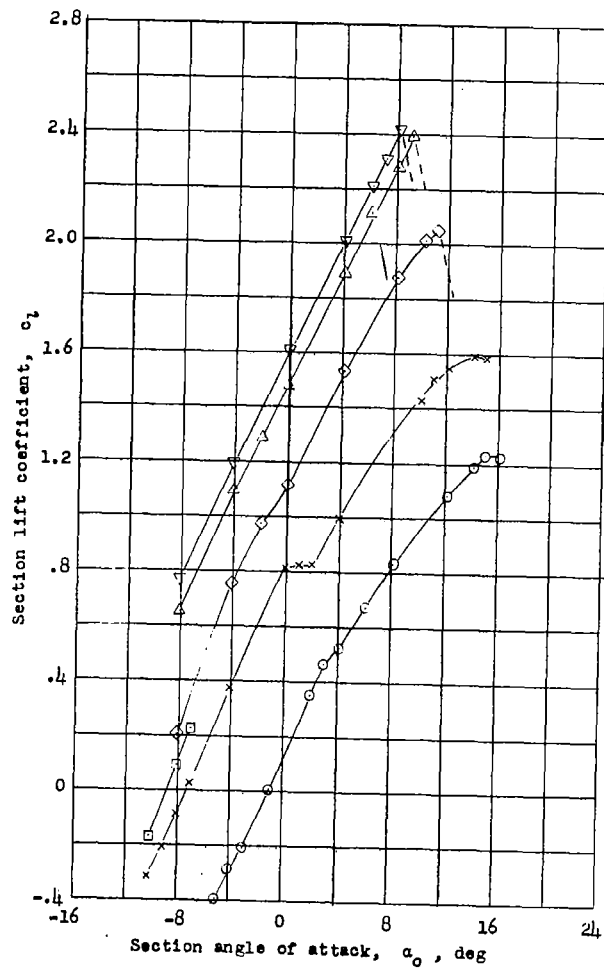
Figure 3 .- Concluded. (d) Pivot point b
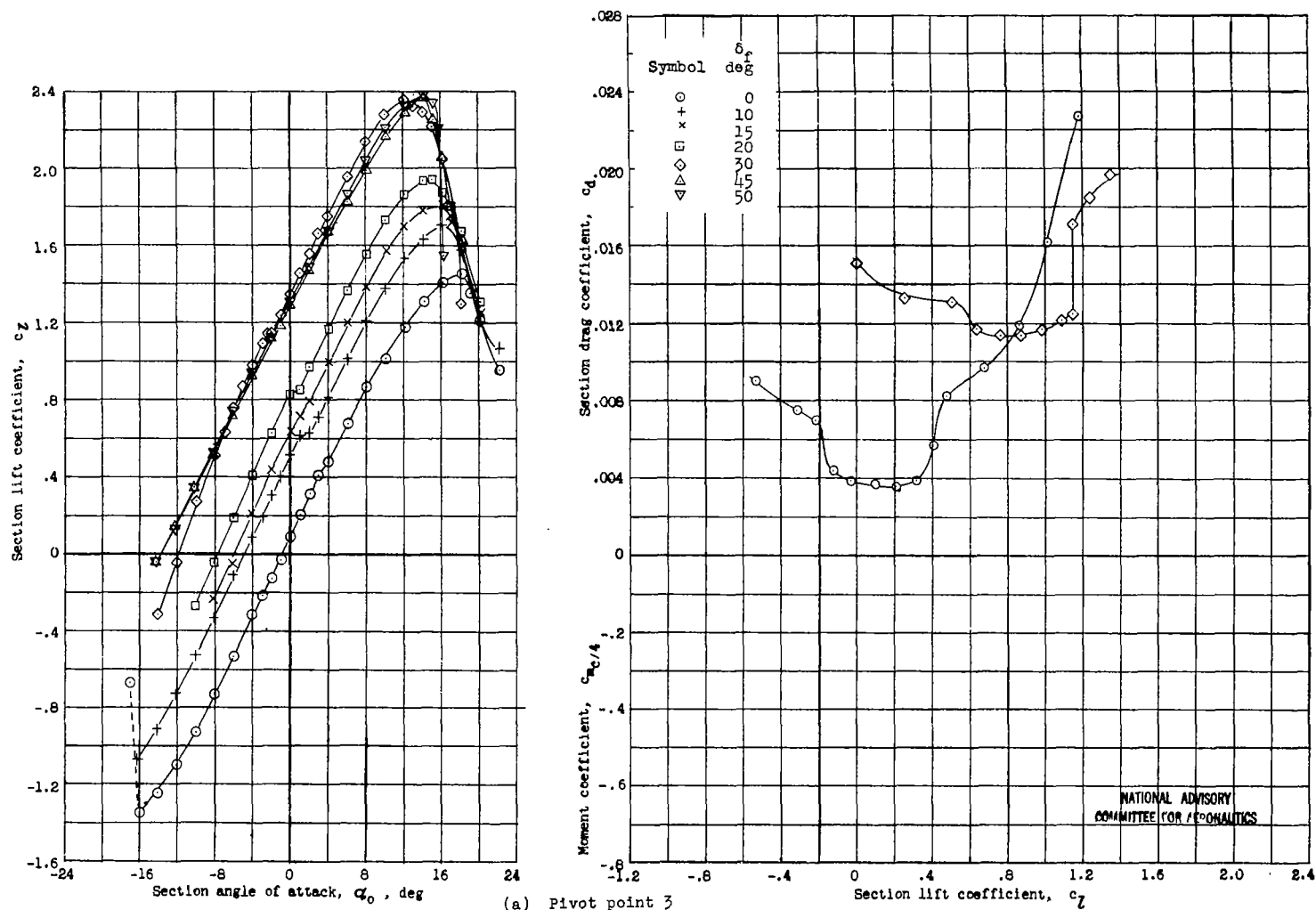
(a) Pivot point 3

Figure 4.- Aerodynamic characteristics of an NACA 66(215)-116, a = 0.6
airfoil with a 0.25-chord slotted flap using various pivot points;
normal operating configurations; R, 6 × 10⁶.
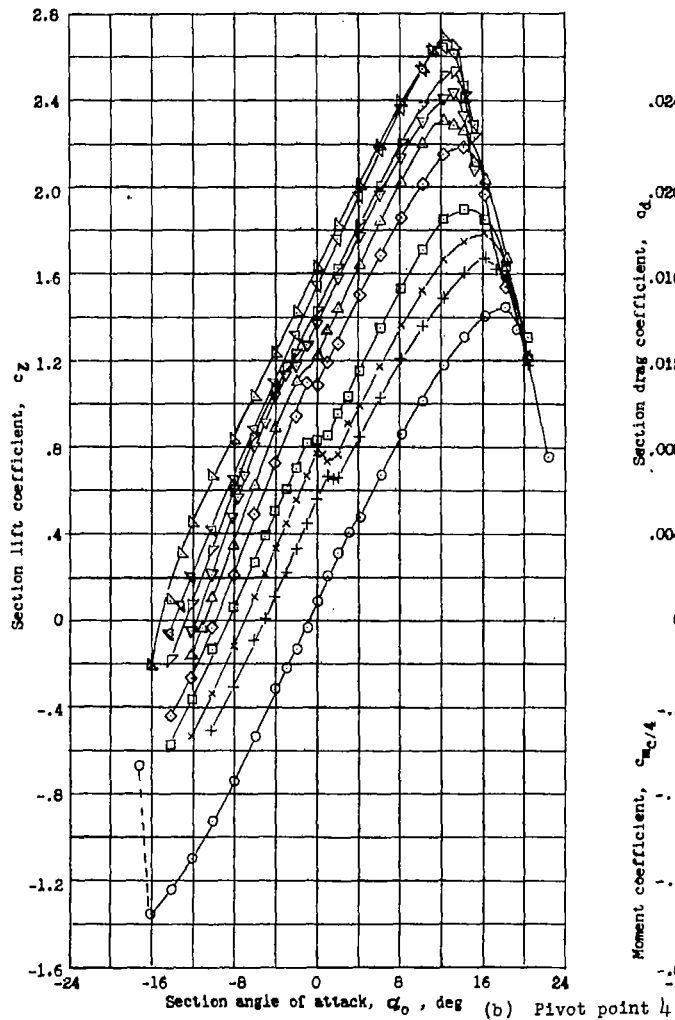
Figure 4 .- Continued

Figure 4.- Concluded

(c) Pivot point 5

Section lift coefficient, c_l

Section angle of attack, a_o, deg

Section drag coefficient, c_d

Moment coefficient, $c_{m_{c/4}}$

Section lift coefficient, c_l

Symbol	δ_f deg
⊙	0
+	10
×	15
⊡	20 (gap sealed)
◇	30
▷	45
◁	50
▽	

NATIONAL ADVISORY
COMMITTEE FOR AERONAUTICS
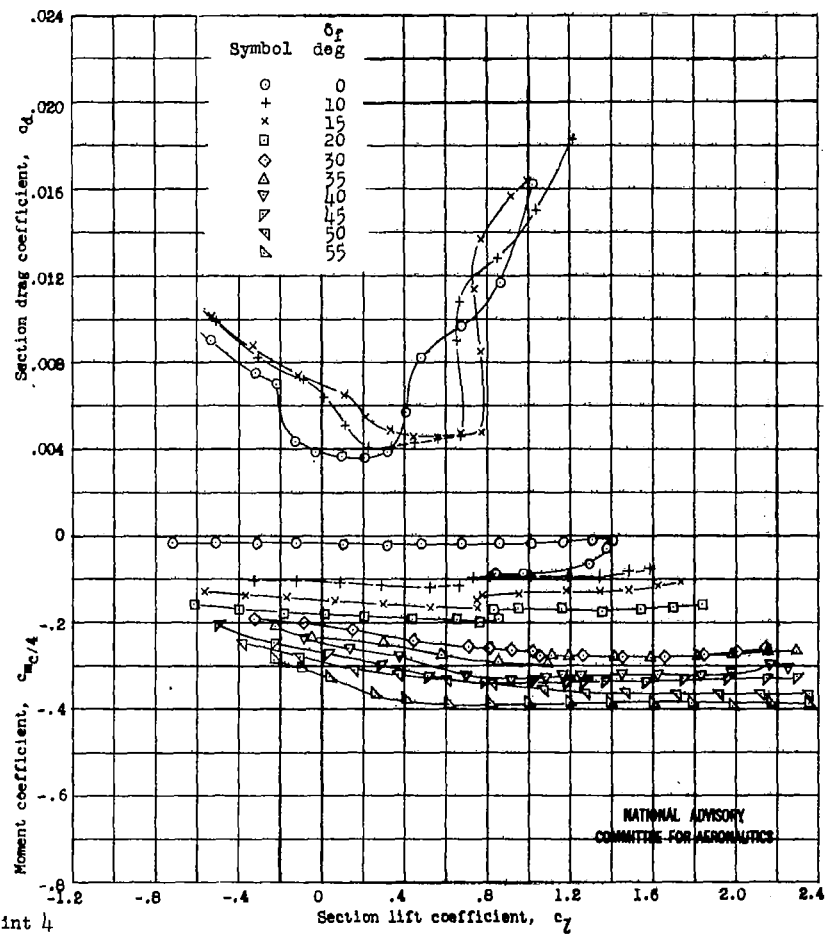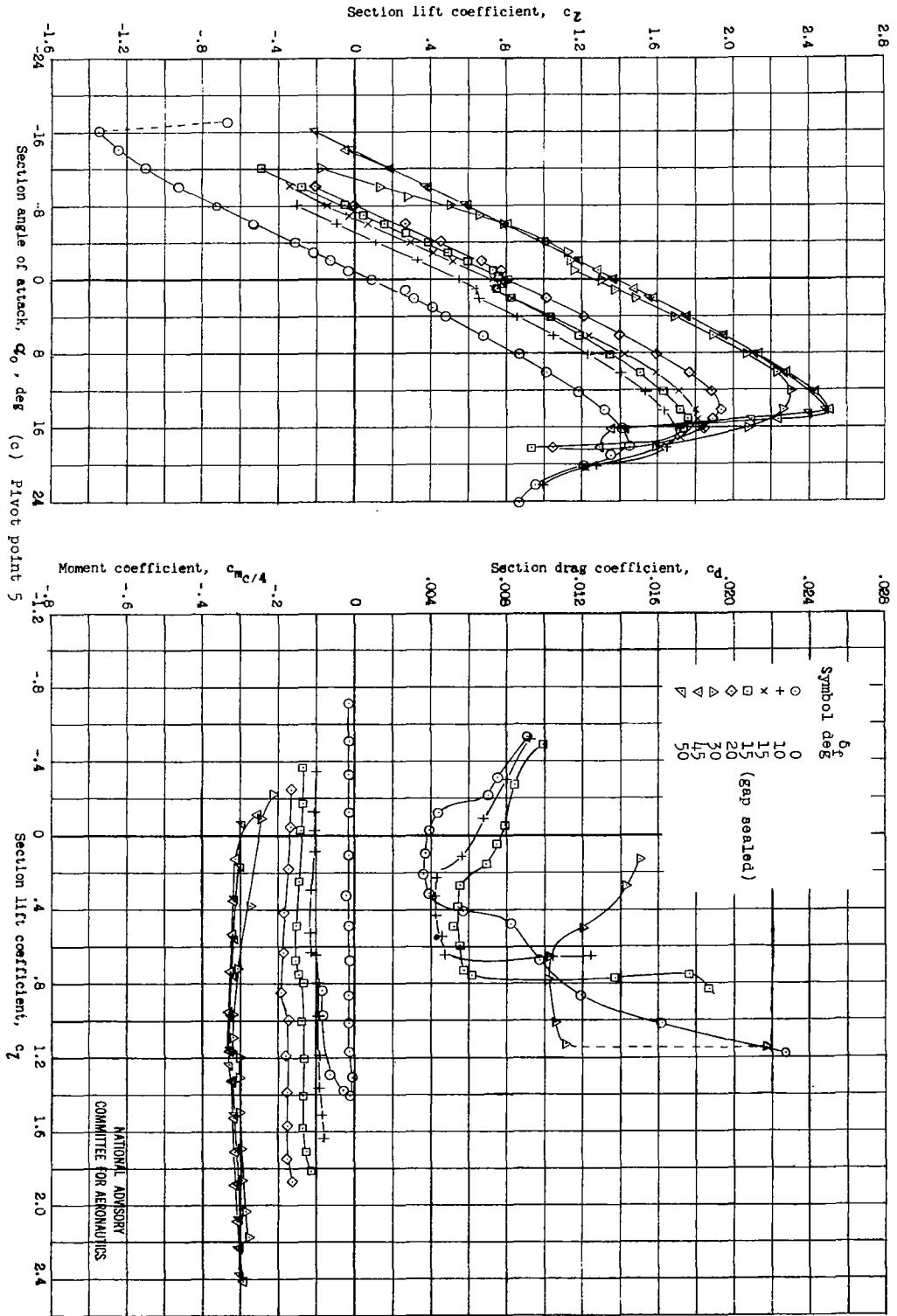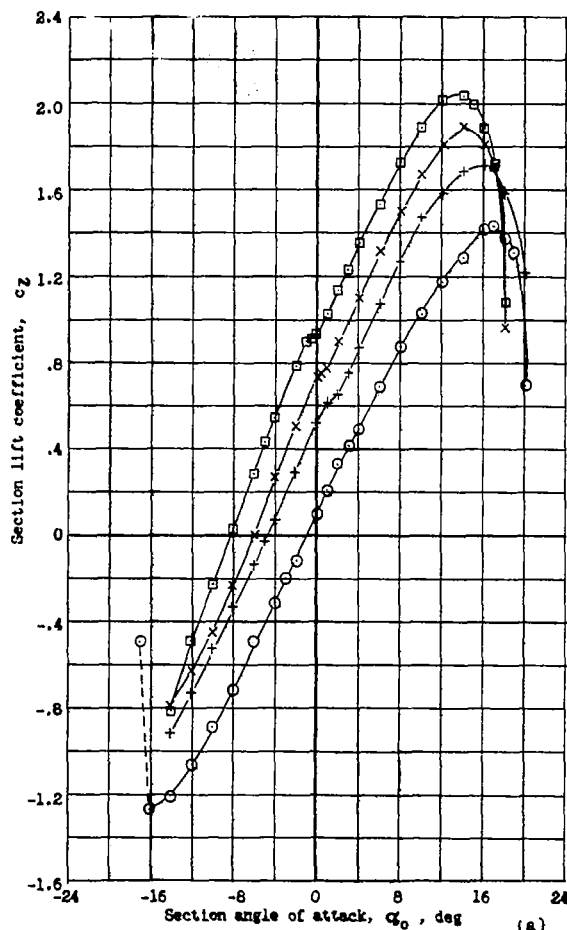
Figure 5.- Lift and drag characteristics of an NACA 66(215)-116, a = 0.6 airfoil with a 0.25-chord slotted flap using various pivot points; low flap deflections with short slot entry lip: R, 6 × 10⁶ (approx.).

Symbol	δ_f deg
○	0
+	10
×	15
□	20

NATIONAL ADVISORY
COMMITTEE FOR AERONAUTICS

Section angle of attack, α_o , deg   (b) Pivot point 4

Section lift coefficient, c_l
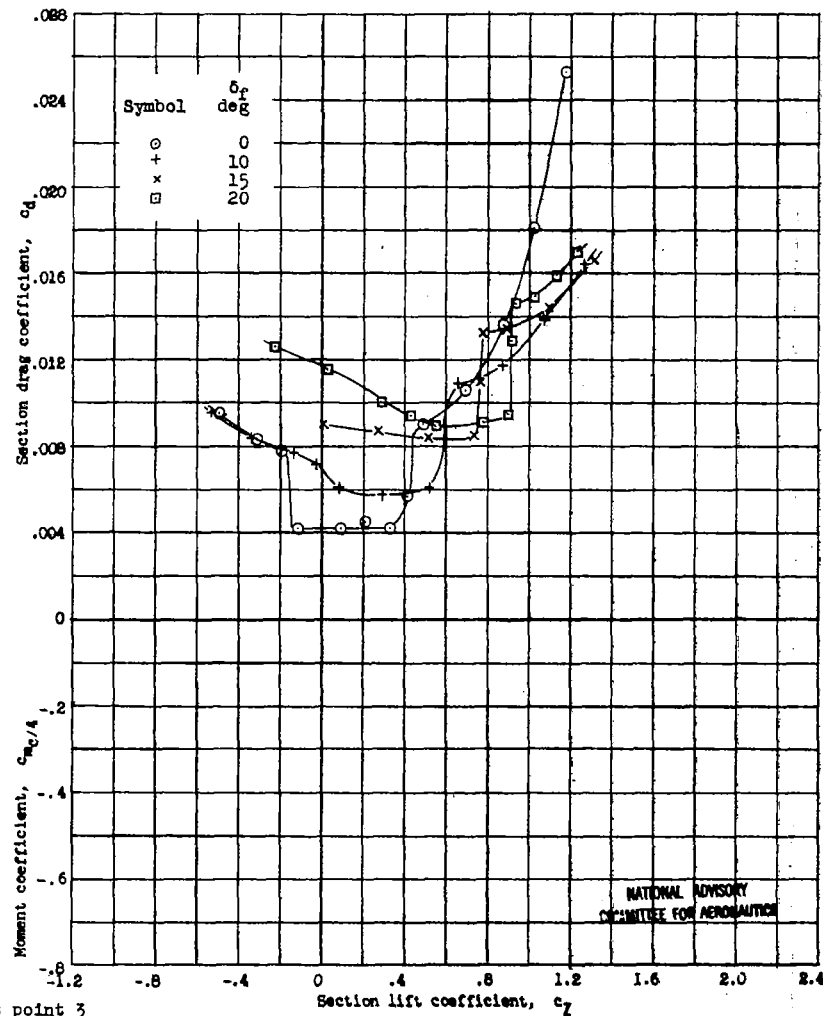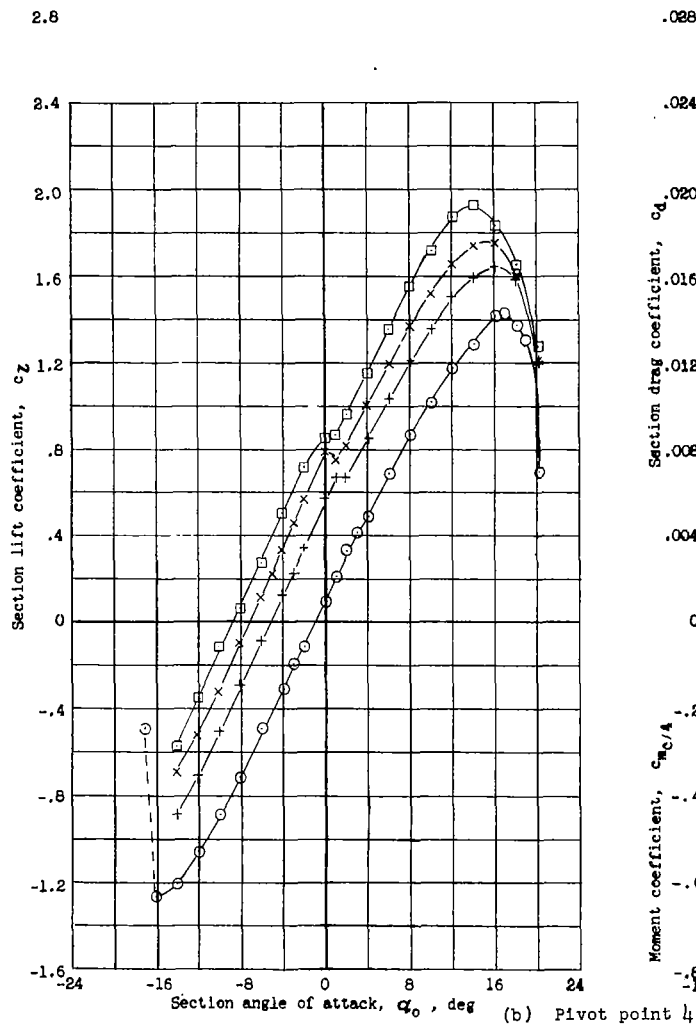
Figure 5 .- Continued
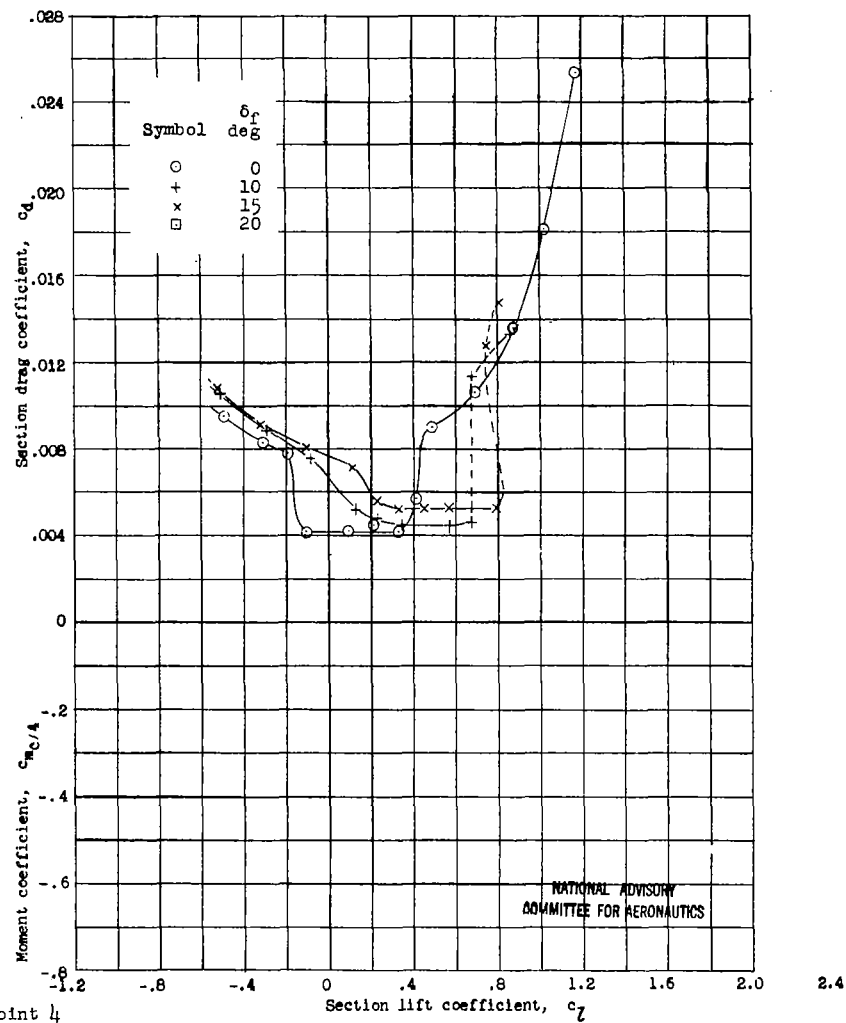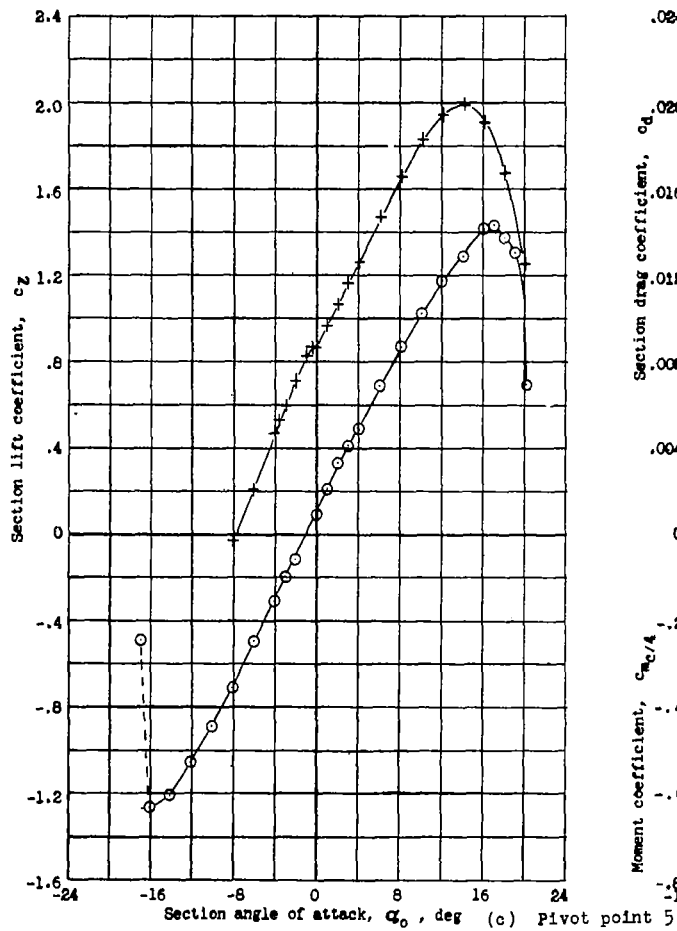
Figure 5 .- Concluded
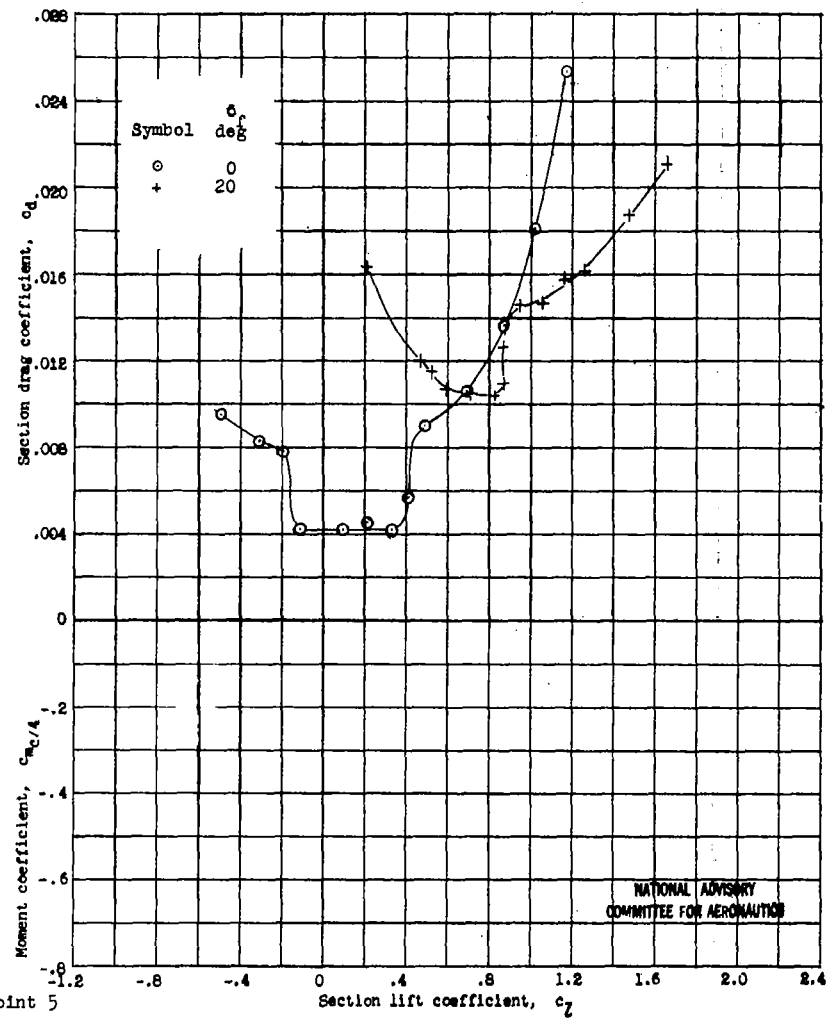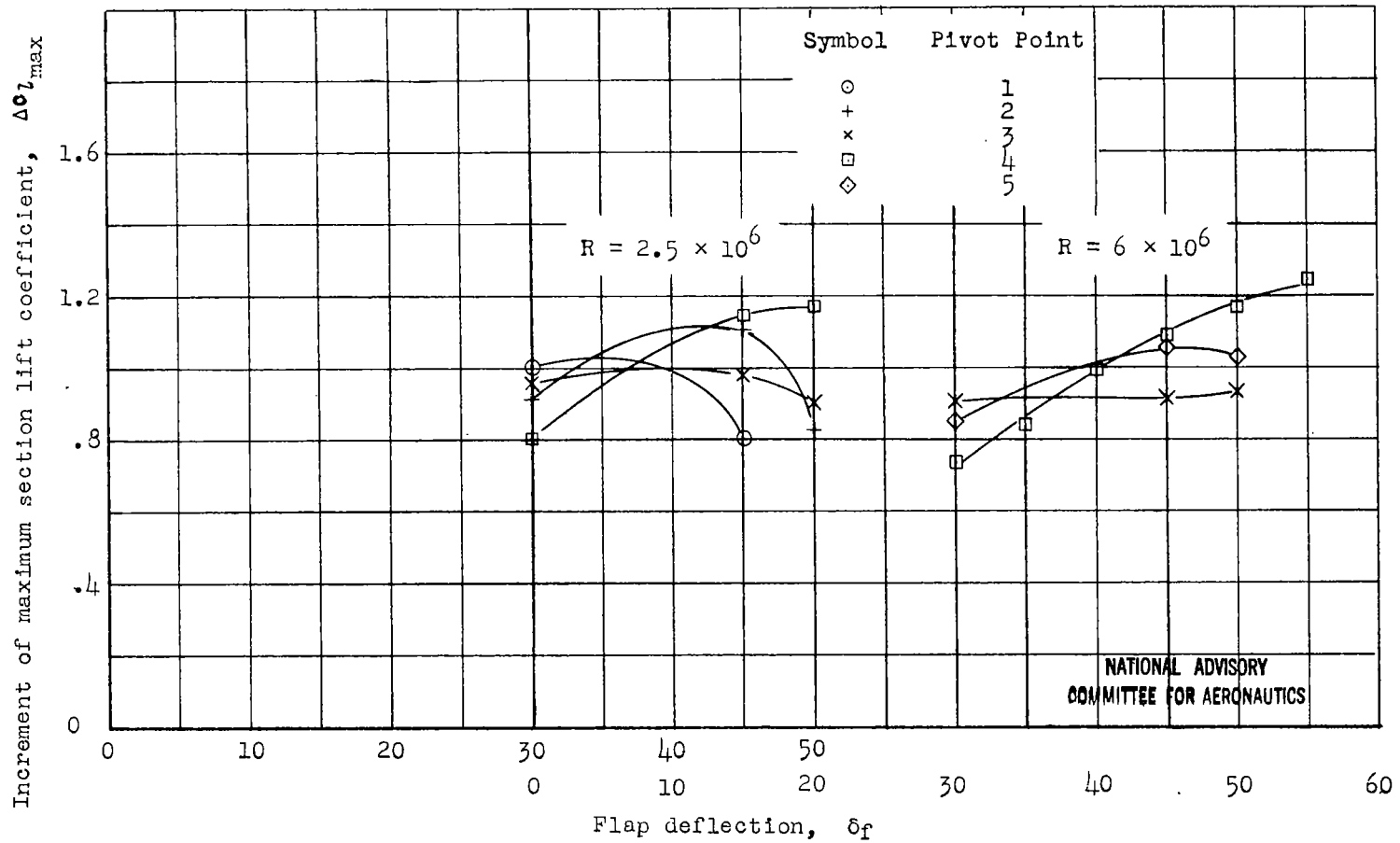
Figure 6 .- Variation of increment of maximum lift coefficient with flap deflection about various pivot points.
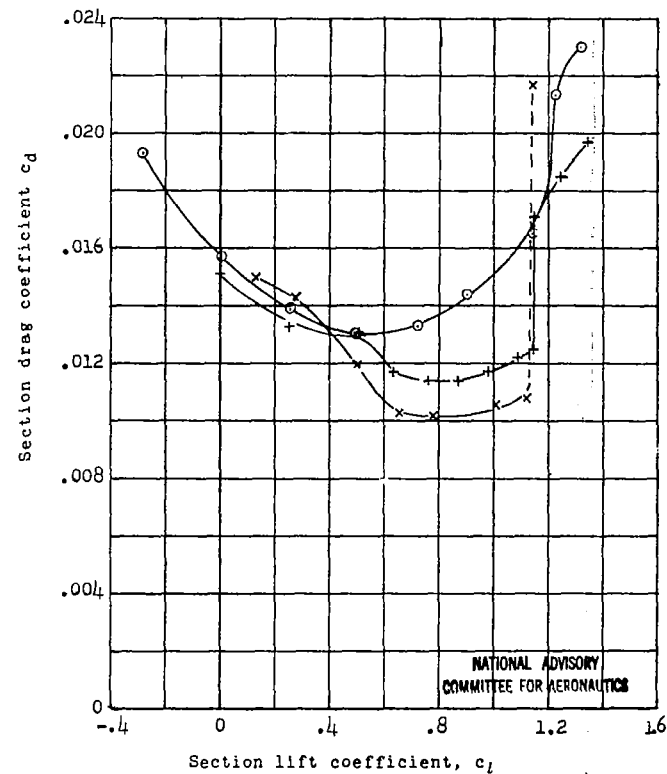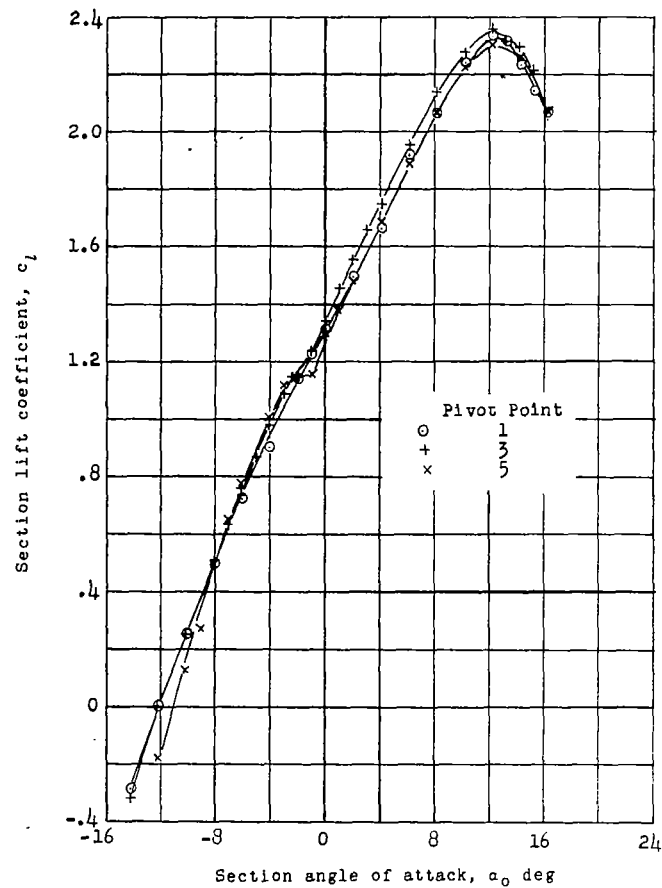
Figure 7.- Variation of lift and drag characteristics for a flap deflection of
30° about various pivot points; short slot entry lip configuration;
R, 6 x 10⁶ (approx.)

$a = 6.09°$ $-7.10°$
$-2.03°$
$3.04°$
$-12.18°$

$30°$

0   0.25   0.50   0.75   1.00

Scale of resultant force vectors   + Pivot point 1
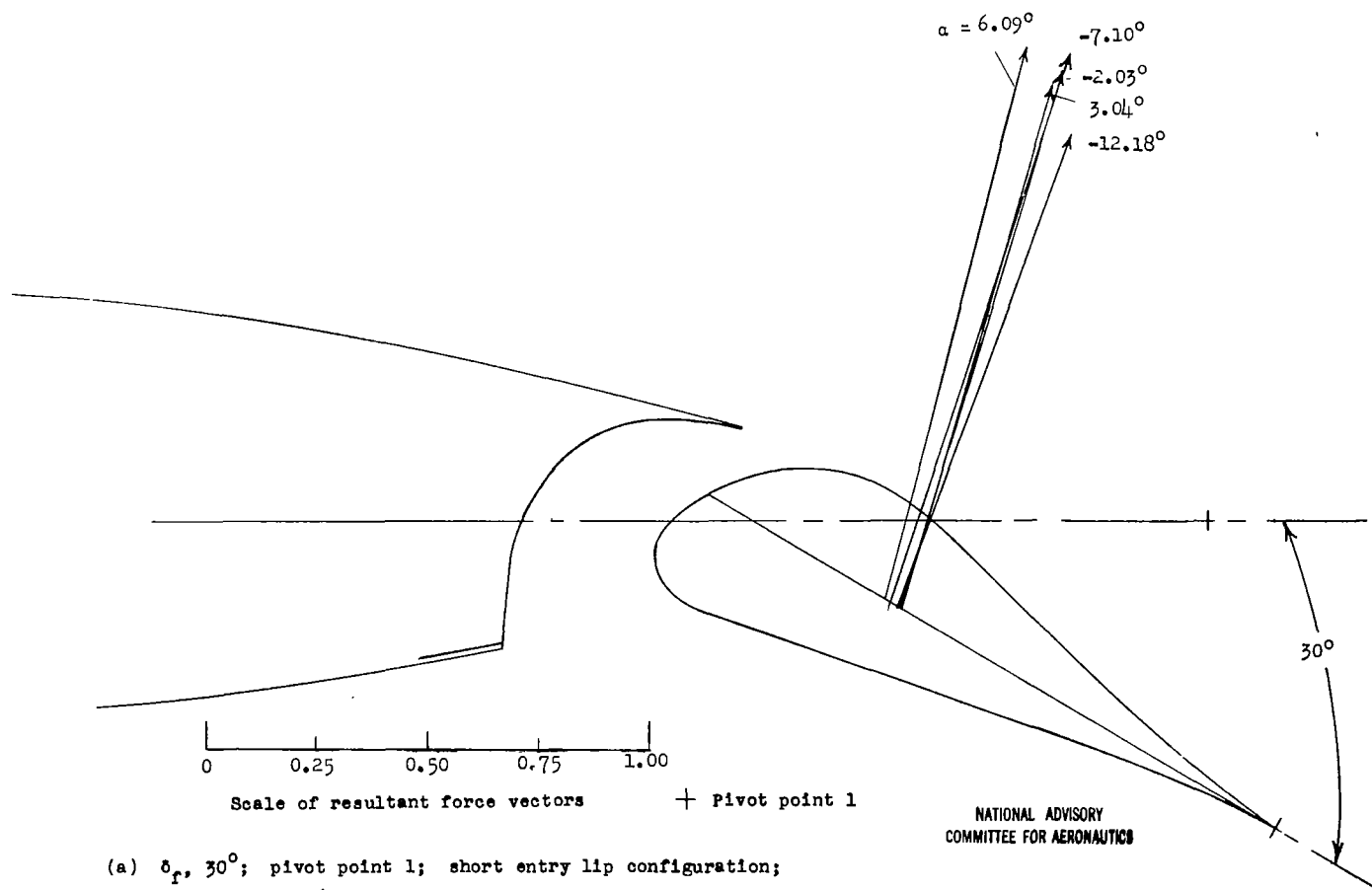
(a) δ_f, $30°$; pivot point 1; short entry lip configuration;

R, 2.5×10^6 (approx.)

Figure 8.- Resultant force coefficient vectors on a 0.25-chord slotted
flap on a 66(215)-116, a = 0.6 airfoil at various angles of attack.

$\alpha = 3.04°$ $6.09°$
$-1.02°$
$-5.08°$
$-10.15°$

NATIONAL ADVISORY
COMMITTEE FOR AERONAUTICS

50°

0   0.25   0.50   0.75   1.00 + Pivot point 4

Scale of resultant force vectors

(b) δ_f, 50°; pivot point 4; short entry lip configuration;
    R, 2.5 × 10⁶ (approx.)

Figure 8 .- Continued

NACA MR No. L4K21

Scale of resultant force vectors ┼ Pivot point 6
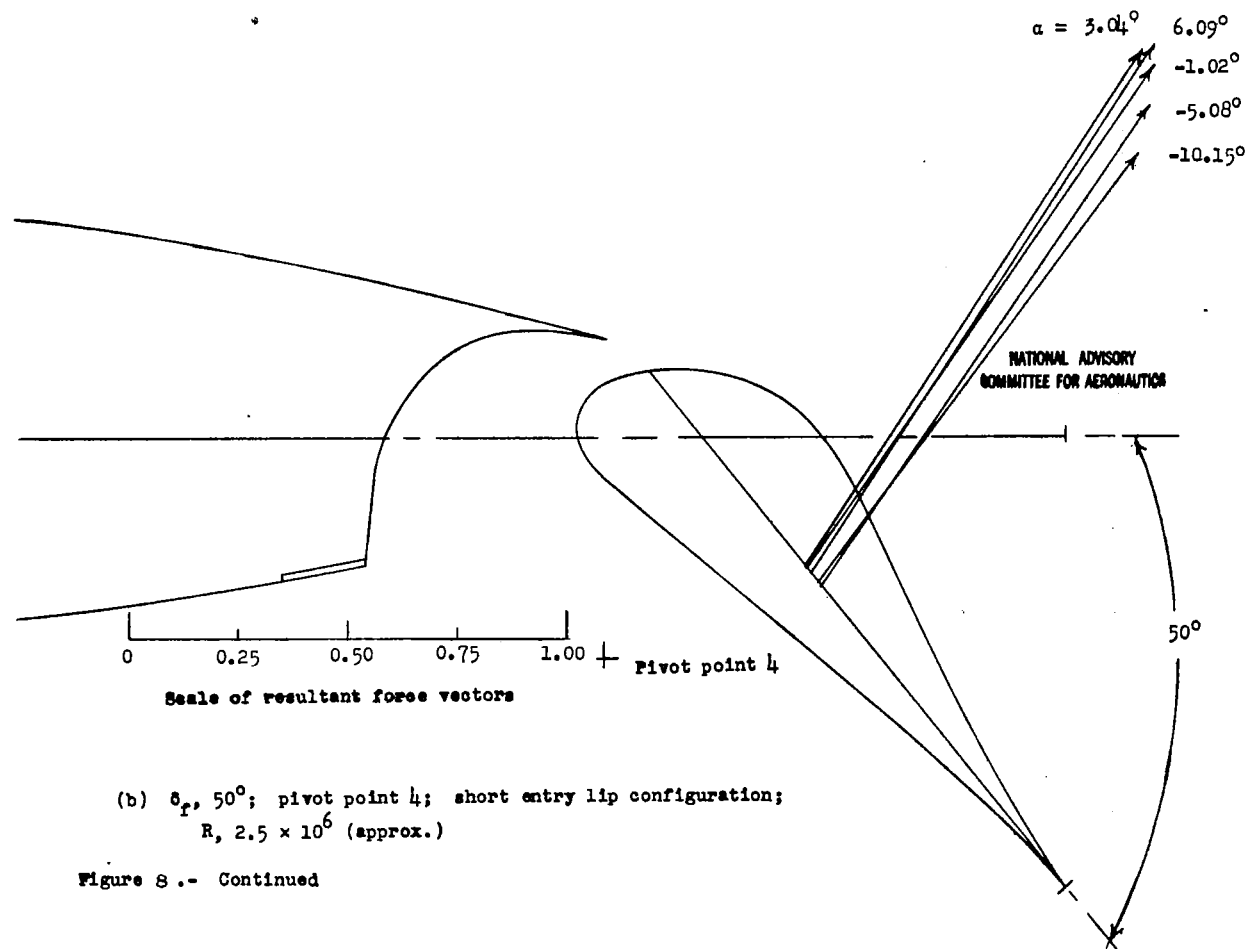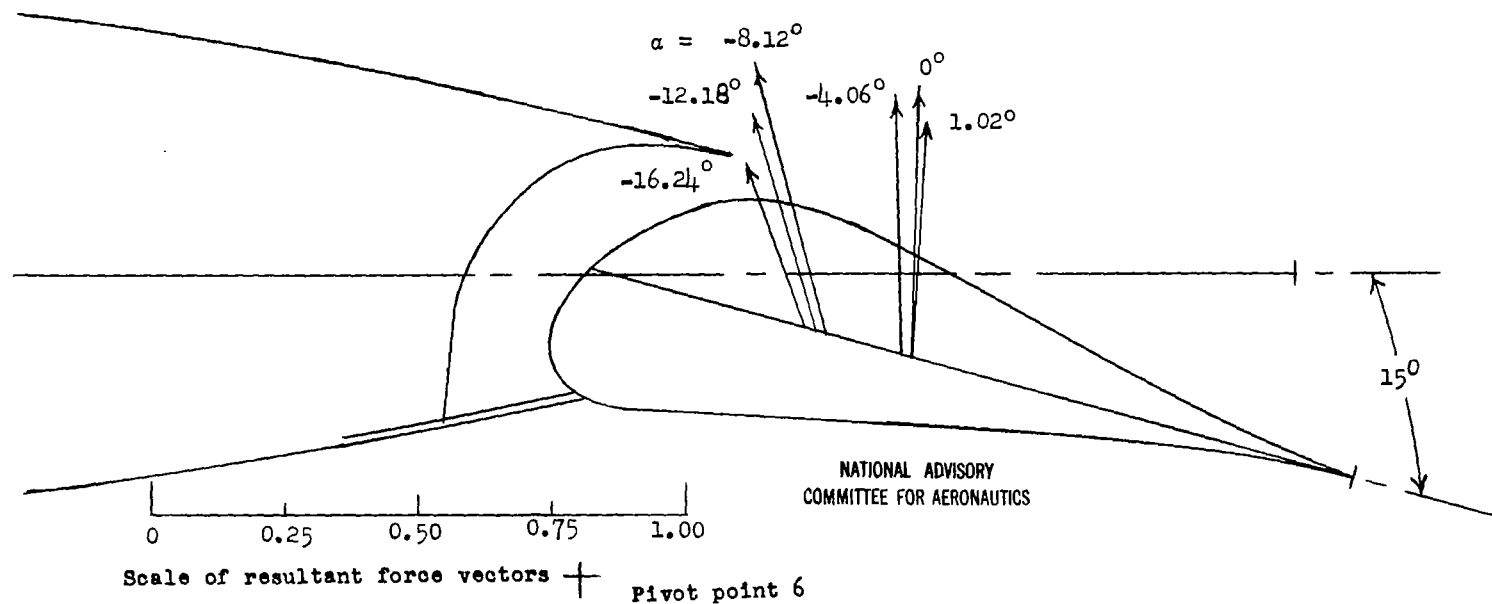
(c) δ_f, 15°; pivot point 6; lower slot gap sealed; R, 6 × 10⁶ (approx.);
    angles of attack from -16.24° to 1.02°

Figure 8 .- Continued

α = 20.30°

16.24°

12.18°

8.12°

4.06°

15°

0   0.25   0.50   0.75   1.00

Scale of resultant force vectors   + Pivot point 6

NATIONAL ADVISORY
COMMITTEE FOR AERONAUTICS
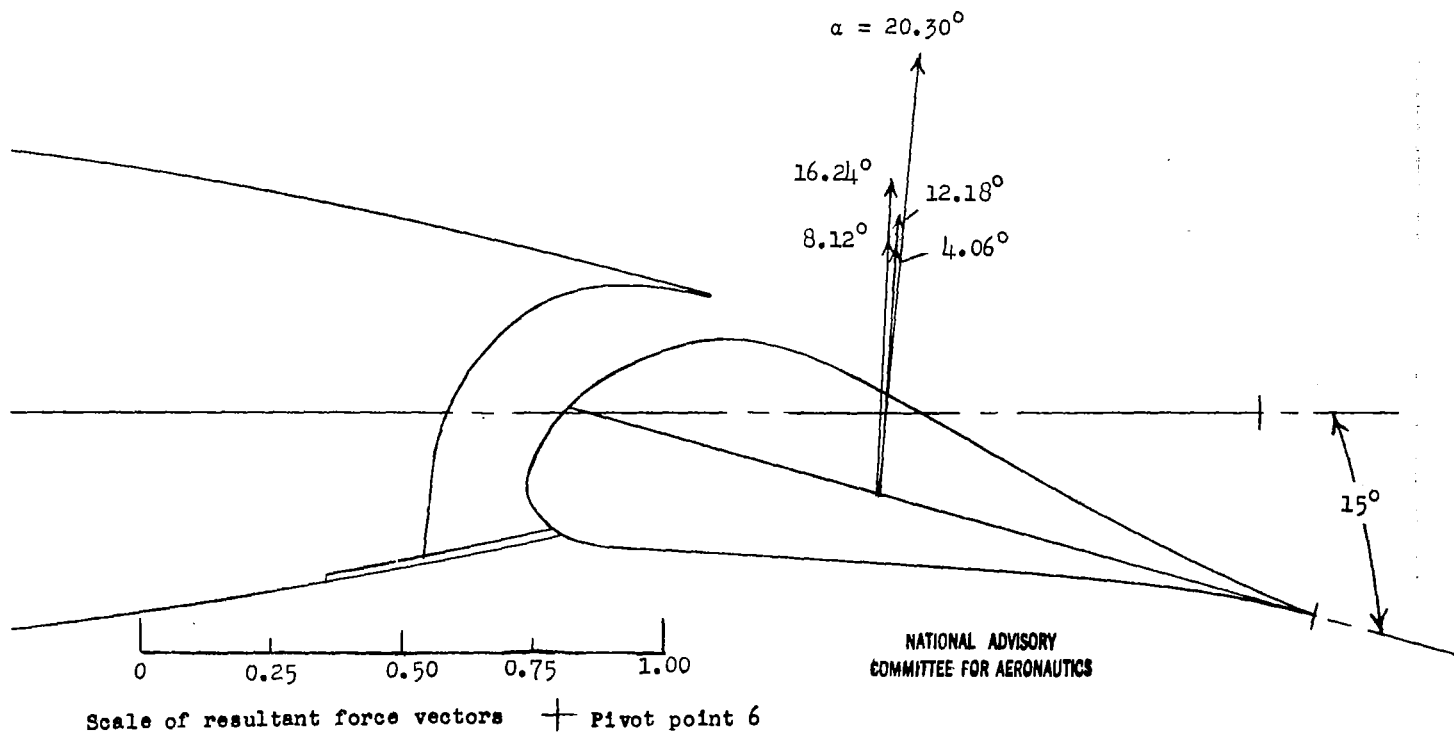
(d) δ_f, 15°; pivot point 6; lower slot gap sealed; R, 6 × 10^6 (approx.);
    angles of attack from 4.06° to 20.30°

Figure 8.- Concluded.
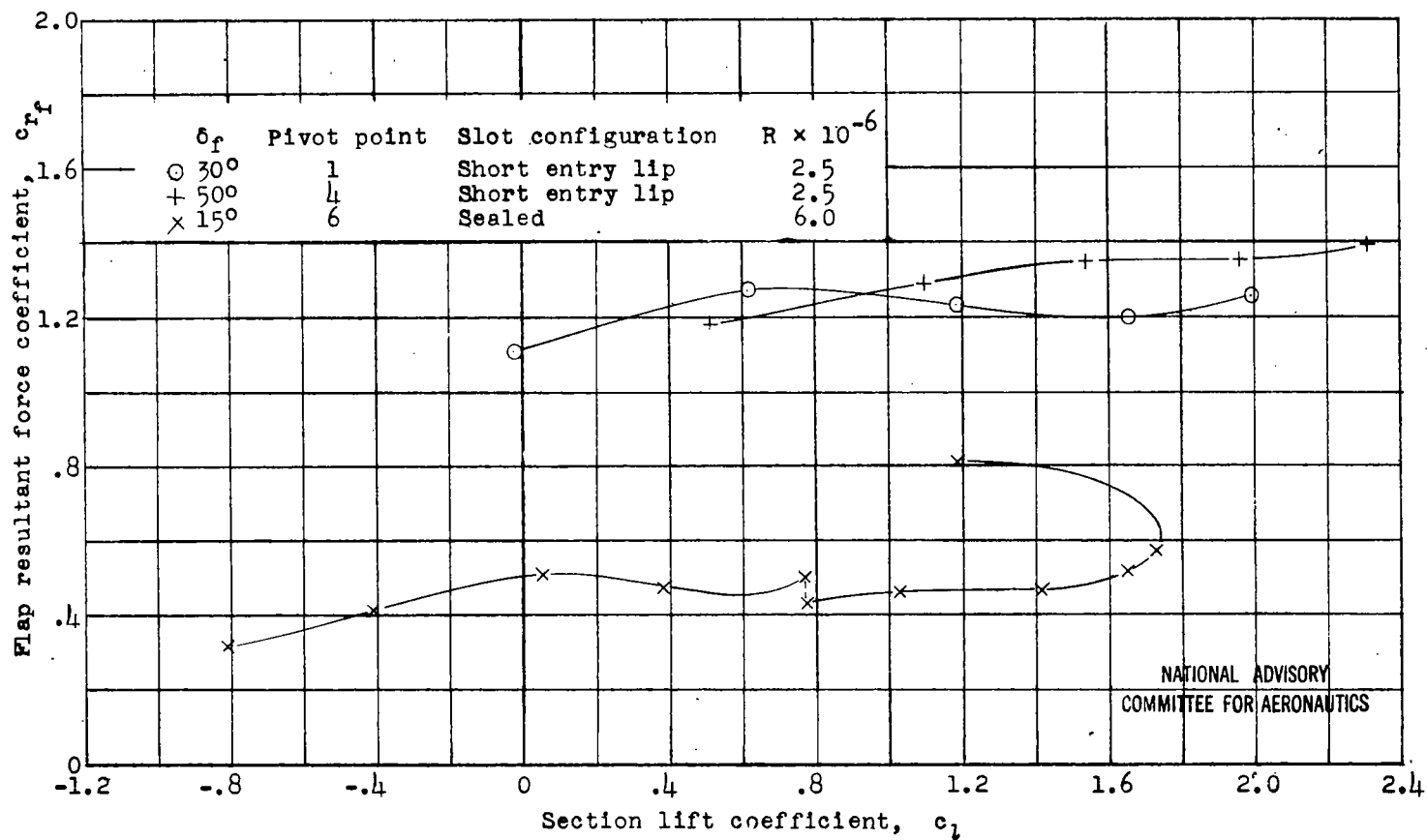
Figure 9 .- Variation of flap resultant force coefficient with section lift coefficient for various flap configurations.

L-629
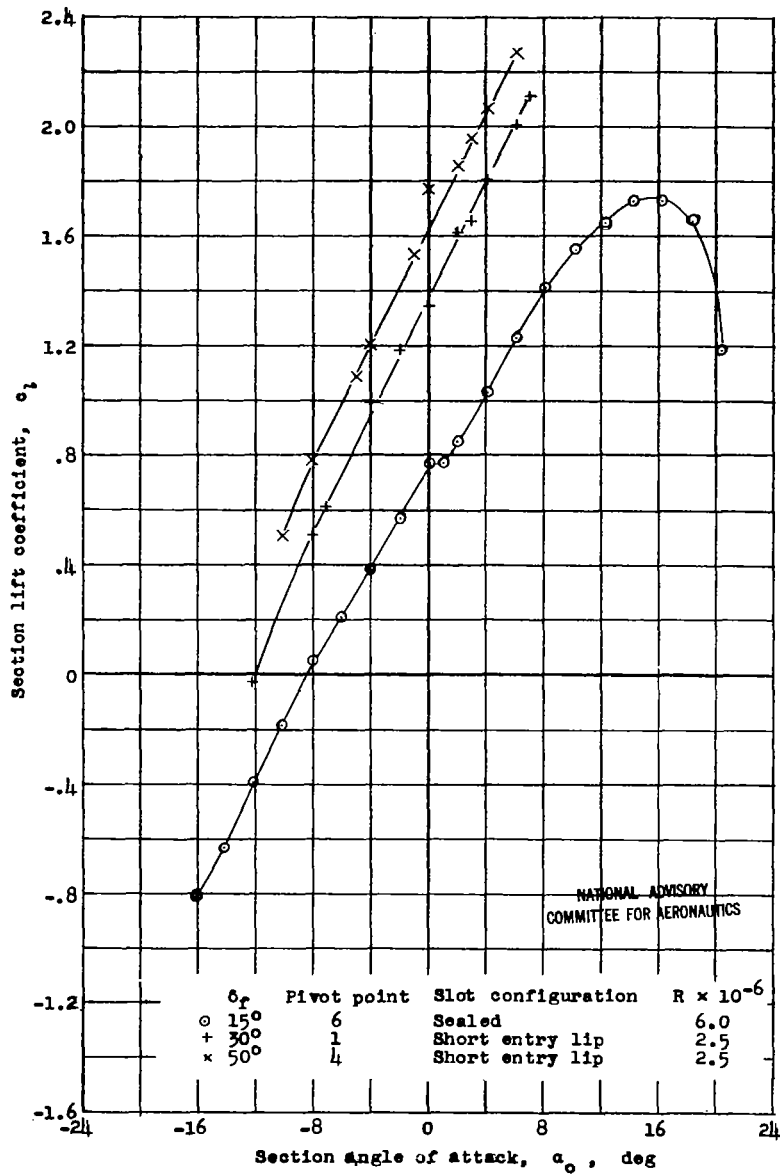
Figure 10.- Variation of section lift coefficient with section angle of attack for various flap configurations.

SECTION B-B

SECTION A-A

NATIONAL ADVISORY
COMMITTEE FOR AERONAUTICS
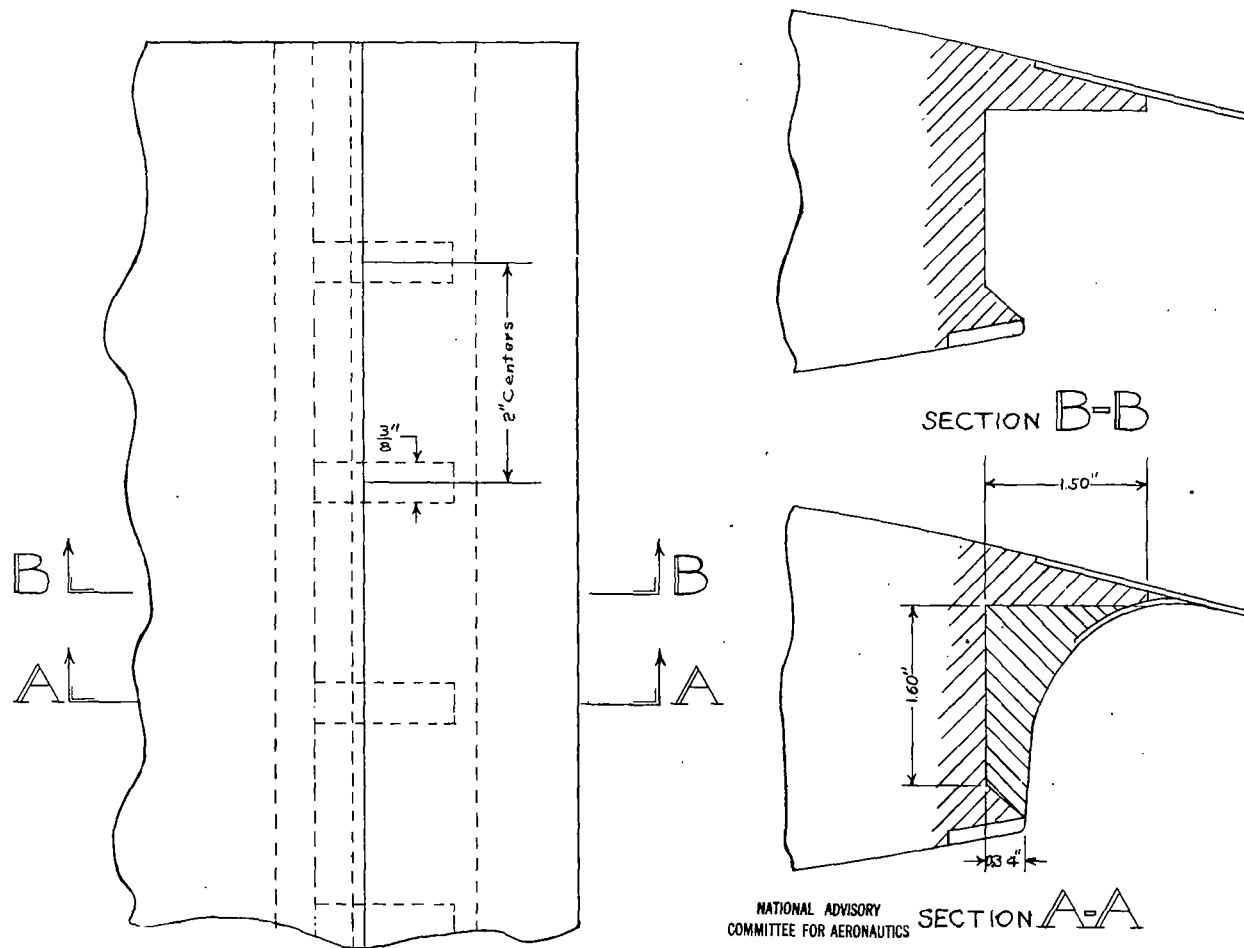
Figure 11.- Slot rework to simulate removal of internal slot fairing skin.
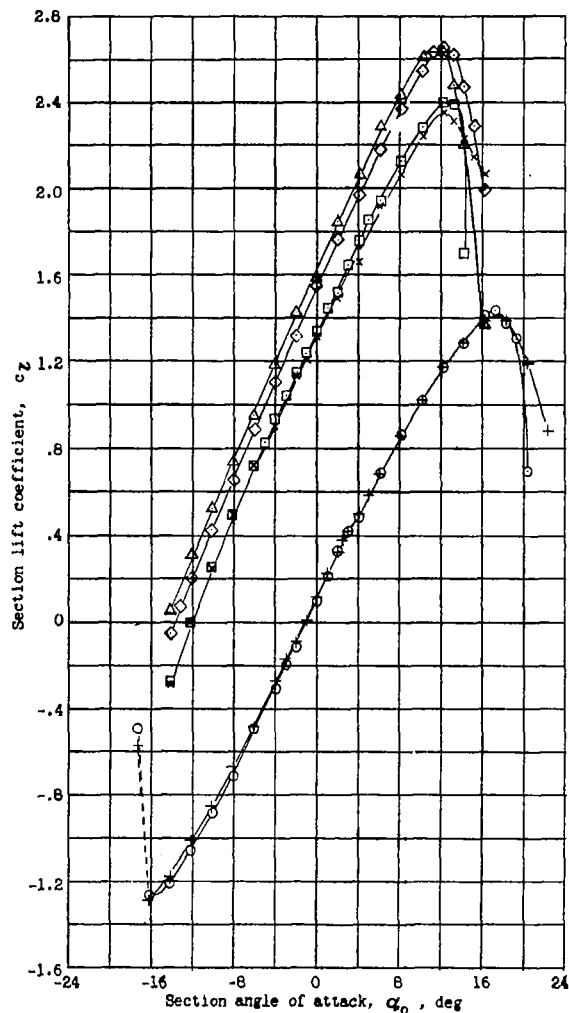
Figure 12.- Aerodynamic characteristics of an NACA 66(215)-116, a = 0.6 airfoil with a 0.25-chord slotted flap; effect of removing internal slot fairing skin, R, 6 × 10⁶.
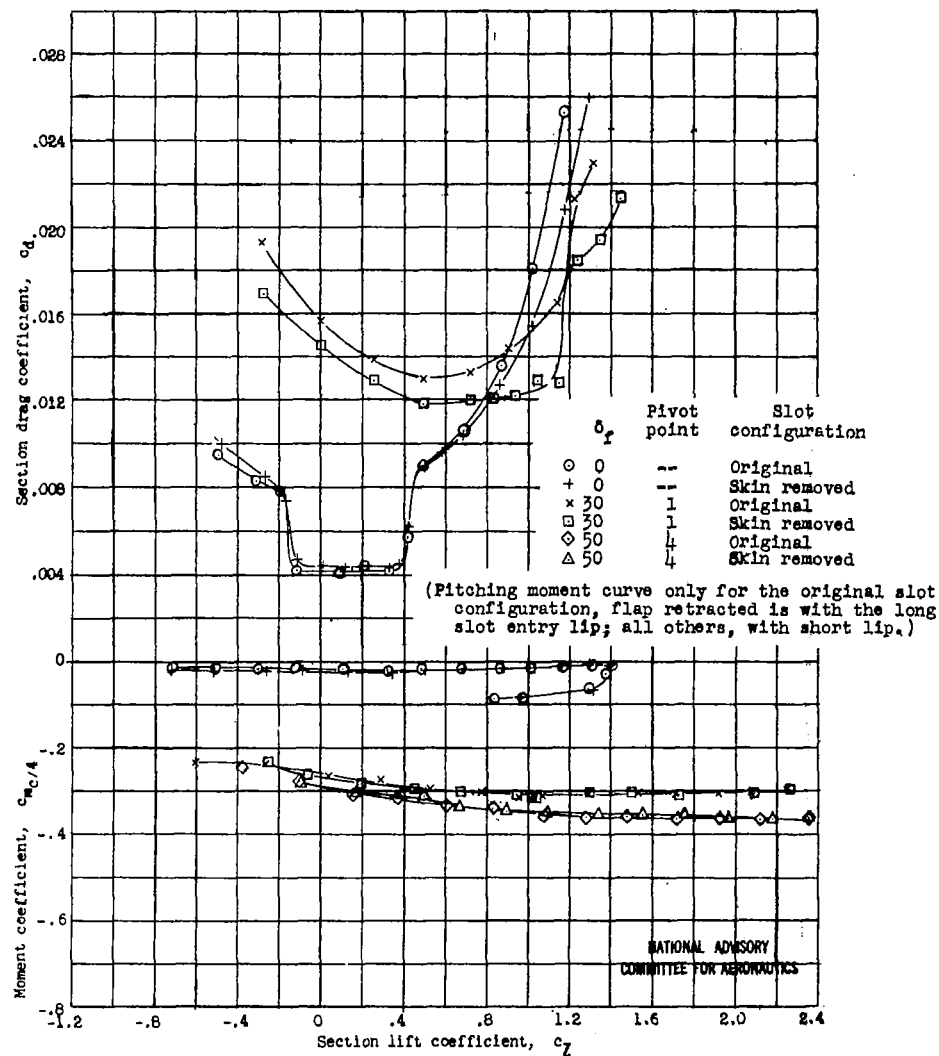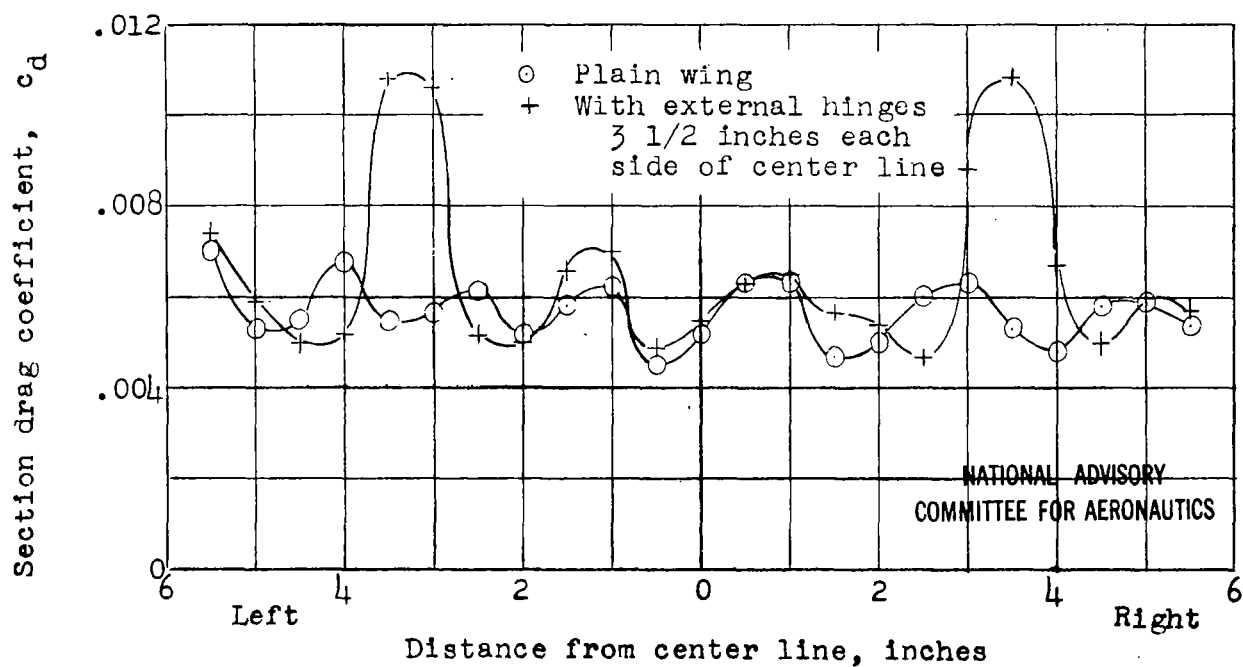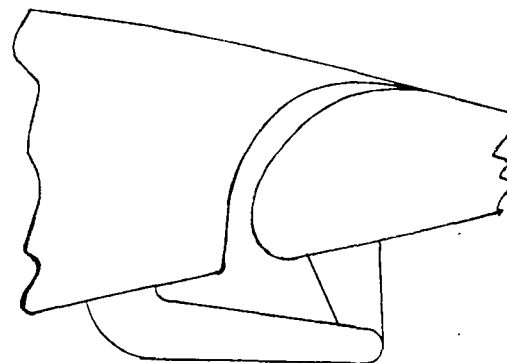
Figure 13.- Spanwise drag surveys with and without external flap hinges. Flap retracted; short entry lip; angle of attack, 1°; R, 2.5 × 10⁶ (approx.).